

NOAA Technical Report NESDIS 102



NOAA Operational Sounding Products From Advanced-TOVS Polar Orbiting Environmental Satellites

Anthony L. Reale
NOAA/NESDIS
5200 Auth Road
Suitland, Maryland 20746

Washington, DC
August 2001

U.S. Department of Commerce
Donald L. Evans, Secretary

National Oceanic and Atmospheric Administration
Scott B. Gudes, Acting Under Secretary

National Environmental Satellite, Data, and Information Service
Gregory W. Withee, Assistant Administrator

1	INTRODUCTION	1
2	BACKGROUND	1
3	ATOVS SCIENTIFIC ALGORITHMS.....	5
3.1	ORBITAL PROCESSING	5
3.1.1	<i>Preprocessing</i>	5
3.1.2	<i>Radiance Temperature Adjustments</i>	5
3.1.3	<i>Contamination Detection</i>	7
3.1.4	<i>First Guess</i>	12
3.1.5	<i>Retrieval</i>	14
3.1.6	<i>Distribution</i>	16
3.2	OFFLINE PROCESSING.....	17
3.2.1	<i>Satellite Radiance Data Sets</i>	17
3.2.2	<i>Satellite and Radiosonde Collocations</i>	17
3.2.2.1	<i>Radiosonde Processing</i>	18
3.2.2.2	<i>Collocation Processing</i>	18
3.2.2.3	<i>The Matchup Database (MDB)</i>	19
3.2.2.4	<i>The First Guess Libraries</i>	20
3.2.3	<i>Coefficients</i>	23
3.2.3.1	<i>Limb Adjustment</i>	23
3.2.3.2	<i>Cloud Detection</i>	23
3.2.3.3	<i>First Guess</i>	23
3.2.3.4	<i>ATOVS-A Retrieval</i>	24
3.2.3.5	<i>ATOVS-B Retrieval</i>	27
3.2.3.6	<i>Radiance Bias (AMSU-B)</i>	27
3.2.3.7	<i>RFI Correction Tables</i>	28
4	RESULTS AND ANALYSIS	28
4.1	VERTICAL ACCURACY STATISTICS	30
4.2	HORIZONTAL FIELDS	30
5	FUTURE PLANS	40
6	SUMMARY.....	42
7	ACKNOWLEDGMENTS	42
	APPENDIX A1.....	43
	APPENDIX A2.....	44
	APPENDIX A3.....	45
	APPENDIX B.....	47
	REFERENCES	51
	LIST OF ILLUSTRATIONS	57
	LIST OF TABLES.....	59

NOAA Operational Sounding Products From Advanced-TOVS Polar Orbiting Environmental Satellites

Anthony L. Reale
NOAA/NESDIS
Washington D.C.

1 INTRODUCTION

The National Oceanic and Atmospheric Administration has deployed and operated a fleet of civilian, polar orbiting, environmental satellites for over 30 years. In 1979, with the launch of the first Television Infra-Red Operational Sounder (TIROS) Operational Vertical (TOVS) configuration onboard NOAA-6, the National Oceanic and Atmospheric Administration (NOAA), National Environmental Satellite, Data, and Information Service (NESDIS) began operating an extensive ground processing capability at Suitland, Maryland to generate and distribute operational TOVS sounding products to users around the world in real time (Werbowetzski 1981). Since then, the NESDIS operational sounding products from polar orbiting satellites have provided a continuous suite of infrared and microwave radiation sounder measurements, and derived temperature and moisture sounding products on a global scale. These data represent a unique source of global, atmospheric, weather information, with a demonstrated positive impact on Numerical Weather Prediction (NWP) forecasts, NOAA's primary mission for sounding products.

The landscape of global weather information from polar orbiting satellites and their application in global weather monitoring and research has undergone significant changes driven by the scientific advances of the past 20 years. This report provides a synopsis of the satellite sounders and derived product systems operated by NESDIS since 1980, followed by a more detailed review of the current radiometers, scientific algorithms and atmospheric sounding products from the Advanced TOVS (ATOVS) sensors onboard the (current) NOAA-15 and 16 satellites, and planned through the year 2010 (NOAA-N').

2 BACKGROUND

The original TOVS sounder configuration onboard NOAA-6 was the first to simultaneously deploy a 20-channel High-resolution Infrared Radiation Sounder (HIRS/1), 4-channel Microwave Sounding Unit (MSU), and 3-channel Stratospheric Sounding Unit (SSU) (Smith et al. 1979) on a global scale. Each was a cross-track scanner¹ center of the scan, and except for some minor changes with HIRS/2 and HIRS/3 versions, this all-weather² configuration of operational, atmospheric radiometers (Kidwell 1998) would remain essentially unchanged until the launch of NOAA-15 in 1998.

The original NESDIS operational sounding products for NOAA-6 were based on a statistical retrieval approach (Smith 1968 and Smith et al. 1976). Soundings were produced per 9x7 array of HIRS fields-of-view (fov), resulting in a nominal horizontal spacing of about 250 km (about double the MSU and over 10 times larger than the HIRS fov). Procedures to compute soundings

¹ Scanning from left to right across the orbit track, with a vertical view (nadir) at the center of the scan.

² MSU measurements penetrate clouds.

included the adjustment of the individual fov across a given scan line to nadir, the spatial interpolation of MSU and SSU fov to the HIRS, and cloud detection and adjustments on the HIRS (McMillin and Dean 1982).

Soundings were derived globally and under all weather conditions (except heavy precipitation). Clear-sky soundings utilized both HIRS and MSU measurements, cloudy soundings the MSU and upper tropospheric HIRS, and both utilized SSU data for stratospheric coverage. The measurements used were averages over the 63 HIRS fov (9x7 array), with clear soundings based on the subset of clear fov (a minimum of five were required to produce a clear sounding), with the sounding location defined at the centroid of averaged fov. Soundings of temperature and moisture were retrieved at pre-defined pressure levels (Kidwell et al. 1998), with the lower twenty levels (1000 to 115 mb) based on regression coefficients which were stratified by latitude and updated weekly, and the upper twenty levels (100 to .1 mb) based on a fixed, initial set of global coefficients (Werbowetzki, 1981). Coefficient updating was based on collocated radiosonde and “clear” satellite observations, which were compiled and updated daily³.

Sounding products were distributed internally to NOAA’s National Meteorological Center (NMC), now the Environmental Modeling Center (EMC), for assimilation into operational NWP (primarily in the northwest Pacific region), and over the Global Telecommunications System (GTS). GTS distribution was at a degraded 500 km horizontal spacing. All products were archived at the National Climatic Data Center (NCDC) (Kidwell 1998). NESDIS quality control was minimal, restricted to gross error checks on the measurements and derived products, and a joint NESDIS/NMC graphic and interactive editing system which provided some quality control of NESDIS soundings (primarily in the northwest Pacific region) prior to NWP assimilation. There was little scientific feedback from users outside of NOAA.

The first significant upgrade of the NESDIS operational sounding products occurred in 1986 (Reale et al. 1986). This upgrade replaced the 9x7 HIRS technique with a 3x3 HIRS technique, including the retrieval of clear soundings at a single HIRS fov (per 3x3) without averaging, referred to as “hole” hunting. Cloudy soundings retained averaging but over the 3x3⁴. The new system also introduced internal quality control based on a recursive filter to identify questionable, bad, and meteorologically redundant soundings. Although the original 500 km spaced products were retained over the GTS, additional product files containing nominal 50 km spaced data more consistent with the radiometric measurements became available. NESDIS also introduced improved quality control, including routine comparisons against operational NWP analysis fields from NMC, and the first in a series of dedicated graphics systems for monitoring and evaluating sounding products (Brown et al. 1988).

The original statistical regression approach for deriving operational sounding products was replaced with a combined physical-statistical retrieval solution in 1988 (Smith et al. 1984 and Reale et al. 1989), including a separate step to compute the first guess profiles (Goldberg et al. 1988). The new retrieval approach combined sets of globally stratified, atmospheric sounder weighting function and vertical covariance matrices (Fleming et al. 1986 and Crosby et al. 1973) to simultaneously retrieve temperature and moisture sounding products. The resulting sets of pre-computed retrieval operators replaced the regression coefficients, retaining the weekly updating

³ Collocation data sets typically spanned the most recent 50-days.

⁴ This was eventually replaced with single fov soundings in 1988.

based on the collocated radiosonde and “clear” satellite observations⁵. Modifications above 100 mb were particularly notable, with the fixed regressions replaced with combined procedures to construct first guess profiles using a combination of short term and long term climatological mean profiles, followed by a retrieval step consistent with the lower levels. This implementation was also the first time that a global NWP forecast model impact study to sanction an operational upgrade (Dey et al. 1989 and Andersson et al. 1991). NESDIS internal graphical and evaluation support also improved considerably, resulting in a more complete system for operational monitoring (Brown et al. 1991).

The late 1980's also marked a period of increased feedback from users outside of NOAA concerning the impact of polar satellite data in global NWP. This was highlighted by the European Center for Medium Range Weather Forecasts (ECMWF), who after conducting several independent experiments on the impact of NESDIS operational soundings on NWP, provided a series of reports identifying sounding problem areas, particularly for cloudy soundings, and associated negative impacts on NWP (Kelly et al. 1991). These reports resounded within NOAA, and marked the beginning of an extensive, 5-year undertaking by NESDIS to identify and correct problems.

As a result, the early 1990's witnessed a series of upgrades to the NESDIS operational sounding products which significantly reduced the errors reported by users. These began with the introduction of cloudy satellite sounding and radiosonde collocations for computing the first guess and retrievals (Reale 1993) late in 1990, and culminated with the new procedures to use NWP surface layer data from 6-hour, global forecasts (Kalnay et al. 1990) as a discriminator for computing cloudy first guess data in April, 1992 (Reale et al. 1994). As a result, a significant component of the problems reported by the ECMWF was resolved, with positive user feedback (Eyre and Uddstrom 1993 and Kelly et al. 1992). Major advances were also realized in the area of quality control with the deployment of enhanced graphical and evaluation systems for routine operational monitoring (Brown et al. 1992).

Meanwhile, the National Meteorological Center (NMC) of NOAA had embarked on a series of actions which ultimately led to the replacement of the NESDIS operational soundings with derived soundings based on an NWP first guess (Daniels et al. 1988) for assimilation into NWP early in 1995. This would be the predecessor of future trends, both nationally and internationally, leading to the direct assimilation of sounder radiation measurements into NWP models in place of derived soundings. The primary motivation for this trend was the reported difficulty (Derber and Wu 1988) in characterizing the background error structures for derived soundings (Sullivan and Gruber 1990) compared to the sounder measurements, as required for the optimal assimilation of observations into NWP (Bergman 1978).

Modification and upgrade of the NESDIS operational sounding products continued through the middle 1990's, impacting almost every aspect of the processing system, but focusing on methods to provide more coherent first guess and derived product background errors, and a more digestible product for NWP assimilation. Upgrades included the expanded use of the HIRS water vapor channels (Wu et al. 1993) for first guess and retrieval (Reale et al. 1995a) in 1993, improved cloud detection (McMillin et al. 1994) in 1994, and numerous refinements in the

⁵ The vertical covariance matrices used were from an independent radiosonde sample (Crosby et al. 1973).

sampling strategies for compiling collocated satellite and radiosonde observations used to compute the first guess and derived sounding products (Reale et al. 1995a).

The final set of changes for operational TOVS product systems, referred to as Revised-TOVS (RTOVS), was implemented into the NESDIS Operations in November, 1997 (Reale et al. 1995b and 1998). Although originally intended as a system upgrade to accommodate a smooth transition to the next generation Advanced-TOVS (ATOVS) sounding systems, RTOVS also included a number of scientific upgrades.

The most notable among the scientific upgrades were the introduction of Advanced Very High Resolution Radiometer (AVHRR) measurements for cloud detection, and a new approach for limb adjustments (Wark 1993). RTOVS also included a more subtle change to the retrieval step, in which the covariance matrix (Crosby et al. 1973) was modified to be based on radiosonde report minus satellite first guess differences, including routine updating (weekly) using the radiosonde and satellite collocations. The result was a more consistent approach for using observed first guess structures in the retrieval solution, a step in the right direction concerning a better characterization of the final derived product background errors.

System changes were also implemented to include both the raw and processed radiometric measurements in the operational data stream, to better accommodate users wishing to assimilate radiance. NESDIS understood that their mission for polar satellite sounding products needed to be expanded to not only provide derived products, but also the radiometric observations now being requested by global users.

On May 13, 1998, the ATOVS instrument configuration onboard NOAA-15 was successfully deployed into a morning orbit (1930 local-time, ascending orbit), followed by NOAA-16 into an afternoon orbit (1400) on September 21, 2000. ATOVS consisted of the new 15-channel Advanced Microwave Sounding Unit-A (AMSU-A), which replaced the MSU and SSU, the new 5-channel AMSU-B for atmospheric moisture, the HIRS/3 and the AVHRR (Goodrum et al. 2000); also see Appendices A1 to A3. ATOVS sounding products from NOAA-15 were operationally implemented by NESDIS in April, 1999 (Reale et al. 1999a and 1999b). This implementation did not include AMSU-B processing which was delayed until May, 2000 (Chalfant et al. 1999 and Reale et al. 2000b).

The deployment of ATOVS also stirred interest among National Weather Service (NWS) field office forecasters concerning the use of polar sounding products in real-time weather forecast applications on a regional (and local) scale. The Polar Orbiting Satellite Sounding Evaluator (POSSE) system (Petty and Brown 2000), a real-time polar satellite sounding data and graphical interface available over the Internet, was implemented in 1999 as a first step toward the inclusion of polar satellite data on the Advanced Weather Interactive Processing System (AWIPS).

The following sections of this report summarize the ATOVS sounding product systems and scientific algorithms operated by NESDIS.

3 ATOVS SCIENTIFIC ALGORITHMS

The scientific procedures for processing NESDIS operational sounding products for ATOVS are presented in the following sections. Two product systems are currently operated, **ATOVS-A**, which processes sounding products using the HIRS, AMSU-A and AVHRR radiometers (Reale et al. 2000a), and **ATOVS-B**, which processes (moisture) sounding products using the AMSU-B radiometer (Chalfant et al. 1999).

The scientific procedures for each system are comprised of two primary subsystems for **Orbital** and **Offline** support processing, respectively. Figure 1 illustrates a generic schematic diagram of these subsystems for ATOVS-A and ATOVS-B, with Orbital processing indicated in red, and Offline processing in green (daily) and blue (weekly).

3.1 Orbital Processing

The orbital processing system outlined in Figure 1 provides:

- Preprocessing
- Radiance Temperature Adjustments
- Contamination Detection
- First Guess
- Retrieval

3.1.1 Preprocessing

Preprocessing steps are done on the raw, level-1b satellite data (Goodrum 2000), which contain the earth located raw satellite measurements from each sounder, and corresponding calibration data, coefficients and quality flags. Preprocessing steps include the application of the calibration coefficients, the computation of the radiance and radiance temperature measurements, quality control, the identification of polar-redundant data (Reale et al. 1999a), and the appendage of ancillary data such as terrain type (Grody 1991 and Grody et al. 1999), sea surface temperature (SST) (Walton et al. 1998) and selected NWP forecast data (Kalney et al. 1990 and Reale et al. 1995).

Preprocessing for ATOVS-A preprocessing step also includes a spatial interpolation of the AMSU-A to the HIRS field of view.

Preprocessing for ATOVS-B includes the correction of AMSU-B measurements for Radio Frequency Interference (RFI) from data transmitters onboard NOAA-15 (Atkinson 1999 and 2000); AMSU-B from NOAA-16 have no RFI. The RFI correction procedures are presented in Appendix B.

3.1.2 Radiance Temperature Adjustments

Limb adjustments are applied to the calibrated, radiance temperature measurements from HIRS/3, AMSU-A and AMSU-B (Wark 1993 and Allegrino et al. 1999), the latter having also been corrected for RFI for NOAA-15. Each of these radiometers is a cross-track scanner, resulting in a systematic variation in the vertical and horizontal sensitivity of each channel across the scan path. Limb adjustments standardize the data from each channel to the vertical (nadir) view, and greatly simplify the subsequent processing of sounding products with little or no degradation in data integrity (Goldberg 1999 and Goldberg et al. 2001).

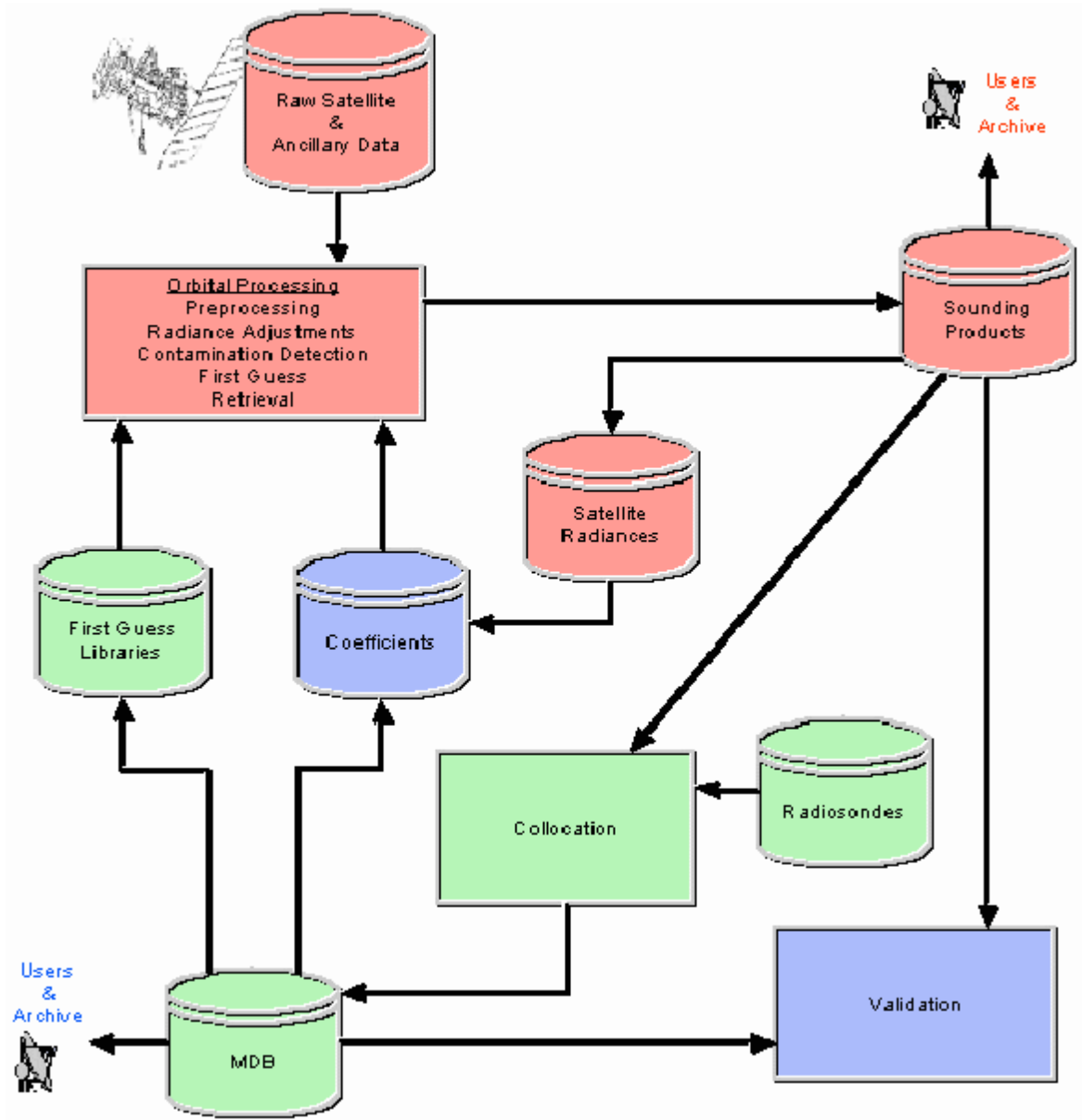


Figure 1: System schematic diagram of Orbital processing (red), and the Daily (green) and Weekly (blue) Offline support systems for ATOVS-A and ATOVS-B sounding products.

The limb (and RFI for NOAA-15) corrected measurements for AMSU-B are also adjusted to remove perceived bias relative to radiative transfer model calculations (Fleming et al. 1991).

Limb and radiance bias adjustments are summarized in Section 3.2.3.

3.1.3 Contamination Detection

Contamination detection is done separately for microwave and infrared sensor data. Microwave contamination detection primarily consists of identifying localized anomalies in AMSU sounding channels sensitive in the lower troposphere⁶, for example AMSU-A channels 4 and 5, typically due to precipitation and large ice particles (Grody et al. 1999). Infrared measurements are screened for clouds.

Precipitation detection and the subsequent editing of AMSU-A and AMSU-B data is done for each fov in the following manner. First, a Cloud Liquid Water (CLW) amount is computed for sea fov, and a Precipitation Index (PI) for land fov, respectively (Grody et al. 1999 and 1994). A median filter analysis is also done for ATOVS-A fov (except high terrain where >1500 m based on AMSU-A channel 4 for sea and channel 5 for non-sea fov, respectively⁷). These results are then combined to identify contaminated AMSU fov. For ATOVS-A, tropical sea fov are flagged if the CLW exceeds 2 mm, extra-tropical (poleward of 30 latitude) sea fov are flagged if both the CLW and median filter difference exceeds threshold⁸, and non-sea fov are flagged if either the PI or median filter exceed thresholds. For ATOVS-B, sea fov are flagged if the CLW exceeds 2 mm, and non-sea fov are flagged based on the PI.

The four panels of Figure 2 illustrate color graphics of ATOVS-A precipitation detection results for NOAA-15 using the above approach. Each panel shows a 6-hour composite field across the Atlantic Ocean and Africa. The upper left panel illustrates CLW values, followed in a clockwise order by the median filter results, the final edit flag, and the corresponding, limb-adjusted, measurements (°K) for AMSU-A channel 5. The bright green areas for CLW indicate values which exceeded the 2.0 mm threshold for contamination over sea. The median filter panel illustrates green and yellow areas, corresponding to edited observations based on AMSU channels 4 or 5, respectively, red areas indicating where no testing was done (i.e., due to high elevation), and grey areas with no contamination. The red areas in lower right panel illustrate candidate ATOVS-A sounding locations identified as contaminated. Good consistency is observed among these parameters, and with areas of contaminated AMSU channel 5 measurements, evident across the Tropical Atlantic and Central Africa.

Cloud detection for HIRS measurements in ATOVS-A (Ferguson and Reale 2000) represents a critical stage of the processing algorithm and determines whether the infrared data can be used in subsequent first guess and retrieval steps.

Cloud detection consists of a series of tests applied to each HIRS fov, segregated over various terrain and solar conditions. If at least one test exceeds threshold, the HIRS fov is designated as cloudy. Tables 1 and 2 list each test, the corresponding test thresholds (OFF indicates the test is not done), and the constraints under which each test is applied. Table 1 lists the regression based

⁶ The concept of sounding channel sensitivity in the atmosphere is discussed in Section 3.2.3.4.

⁷ The use of channel 4 over sea and 5 over land is consistent with their use in subsequent first guess and retrieval steps.

⁸ The median filter threshold is currently 1.5 K for all tests.

NOAA-15

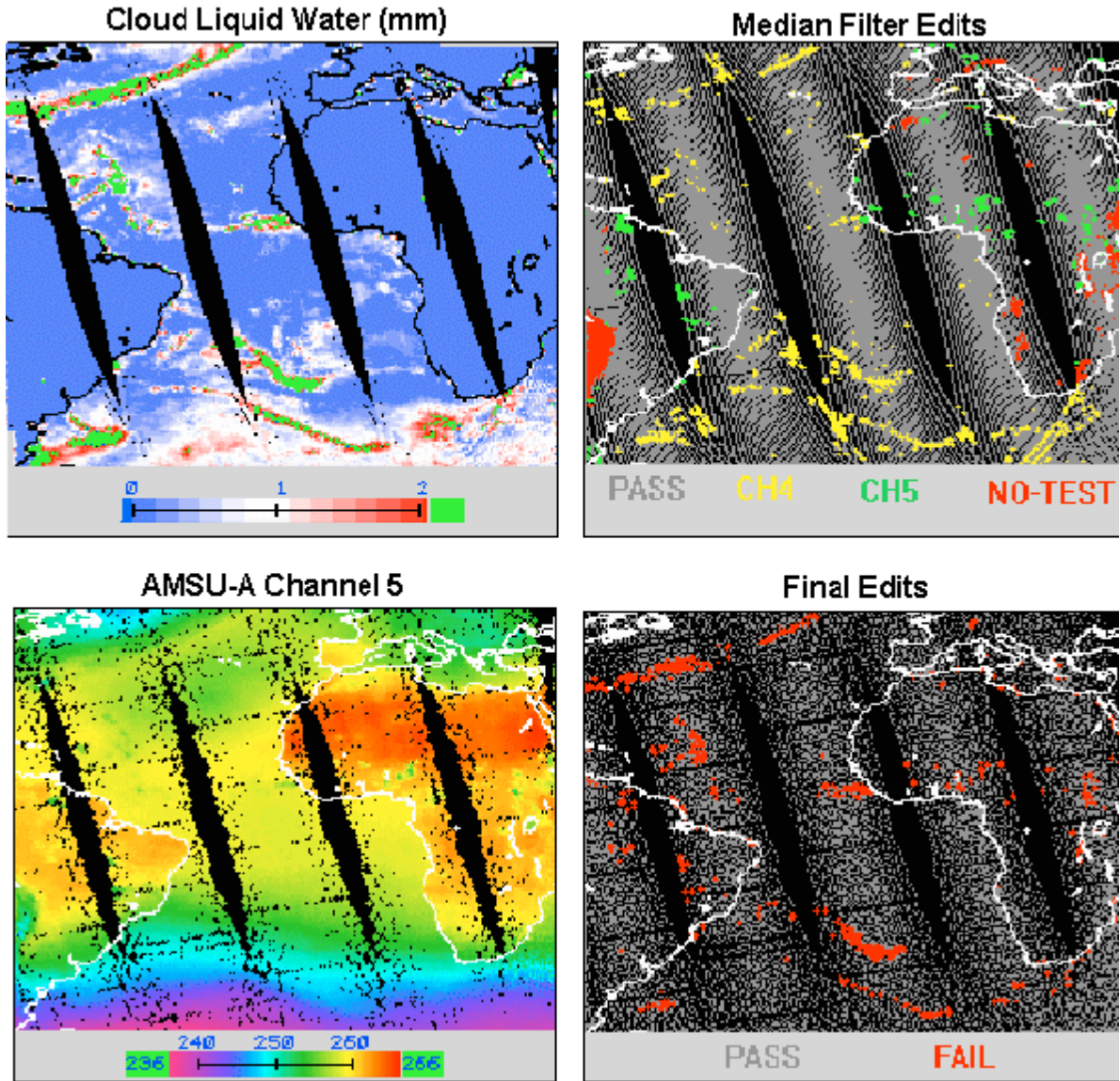


Figure 2: Precipitation detection parameters of Cloud Liquid Water (mm) (upper left) and median filter edits (upper right), the final set of edits for AMSU-A fov (lower right), and AMSU channel 5 radiance temperature ($^{\circ}$ K) measurements (lower left), composited from 16Z to 23Z on September 6, 2000 for NOAA-15.

tests, and Table 2 the remaining tests, including restoral and adjacent spot tests. Although fairly constant over time, the test thresholds require routine monitoring and are adjusted as necessary to maintain a consistent global mask throughout the year.

The prefixes “STE” and “P” in Tables 1 and 2 refer to Surface Temperature Estimates and Predicted parameters, respectively, and are determined using regression coefficients as presented later in Section 3.2.3.2. SST refers to the NESDIS operational sea surface temperature products (Walton et al. 1998), which are appended to each HIRS data record during orbital preprocessing. AVHRR tests consider each of the 17 Global Area Coverage (GAC) (Kidwell 1998) pixels centered on the HIRS fov, and if one (or more) fails the HIRS fov is designated as cloudy⁹.

Regression Test	Threshold	Constraint
STE _{H8}	270 °K	SEA, DAY
STE _{H18}	270 °K	SEA, NIGHT
STE _{H18} - STE _{H8}	OFF	DAY
	OFF	NIGHT
STE _{H19} - STE _{H18}	OFF	NIGHT
STE _{H8} - HIRS ₈	± 6.0 (°K)	SEA, 30N TO 30S
	± 5.0	SEA, POLEWARD 30N, 30S
	± 4.0	SEA-ICE
	± 5.0	LAND
	± 4.0	SNOW COVER
SST - STE _{H8}	< -10, > 2.0 (°K)	SEA, DAY
SST - STE _{H18}	< - 5 , > 1.5	SEA, NIGHT
PAVHRR3 - AVHRR3	OFF	NIGHT
PAVHRR4 - AVHRR4	< -2.0, > 1.5 (°K)	SEA
	< -0.2, > 5.0	SEA-ICE
	< -0.2, > 2.5	LAND
	< -0.5, > 5.0	SNOW COVER
PHIRS7 - HIRS7	OFF	NIGHT
PAMSU5 (LW) - AMSU5	± 5.0 (°K)	NONE
PAMSU5 (SW) - AMSU5	OFF	NIGHT
PAMSU7 (LW) - AMSU7	OFF	NONE
PAMSU7 (SW) - AMSU7	OFF	NIGHT

Table 1: Regression based cloud detection tests, thresholds and application constraints for ATOVS-A, NOAA-15, during September-2000¹⁰. The prefixes “STE” and “P” refer to Surface Temperature Estimates and Predicted parameters.

⁹ The exceptions are tests of the Standard Deviation, and percent of the (17) GAC pixels which exceed 270 K, based on AVHRR channel 4.

¹⁰ Thresholds for a given test can vary per satellite and over time.

Test	Threshold	Constraint
ALBEDO: (HIRS20)	OFF	DAY; LAND (NO SNOW/ICE)
ALBEDO: (HIRS20)	OFF	DAY; SEA
AVHRR4 - AVHRR3	< -5.0, > 0 (°K)	NIGHT
% AVHRR4 (> 270)	OFF	NONE
ST. DEV. AVHRR4	> 4.5 (°K)	NONE
RESTORAL: (STE8)	> 310 (°K)	LAND
ADJACENT SPOT:		
ISOLATED CLOUDY	NA	NONE
STE8 (ADJ) - STE8	± 5.0 (°K)	NONSEA, DAY
STE18 (ADJ) - STE18	± 5.0	NONSEA, NIGHT
STE8 (ADJ) - STE8	± 3.0	SEA, DAY
STE18 (ADJ) - STE18	± 3.0	SEA, NIGHT

Table 2: Non-Regression, Restoral and Adjacent Spot cloud detection tests, thresholds and application constraints for ATOVS-A, NOAA-15, during September 2000

The Restoral and Adjacent Spot tests listed at the bottom of Table 2 are done after all the other tests are completed. The restoral test, also referred to as the hot-land test, resets a cloudy fov to clear if the “STE8” value exceeds 315 °K. Adjacent spot tests compare clear fov with their eight adjacent (ADJ) neighbors, and resets to cloudy if surrounded by cloudy scenes, or if the threshold is exceeded for at least one pair.

The four panels of Figure 3 show color-enhanced, composite fields of NOAA-15, evening, cloud detection results across the northern and tropical Atlantic. Shown (clockwise beginning upper left) are the measured HIRS channel 8¹¹, the test differences for “SST - STE18”, and for “PAMSU5 (LW) – AMSU5”, respectively (see Table 1), and the resulting cloud mask (lower left). The color scale for each panel is shown below, and for test difference panels are set so that bright green indicates where the cloud threshold was exceeded, or the test not done (i.e., for “SST - STE8” over land). Good consistency is seen among the colder HIRS channel 8 values indicating clouds, the bright green areas where test thresholds were exceeded, and the resulting cloud mask.

Global cloud cover represents an important component of weather information provided by the polar satellites. Typically, about 65% of the total number of HIRS fov are declared cloudy.

¹¹ HIRS channel 8 is an atmospheric window channel sensitive to clouds.

NOAA-15

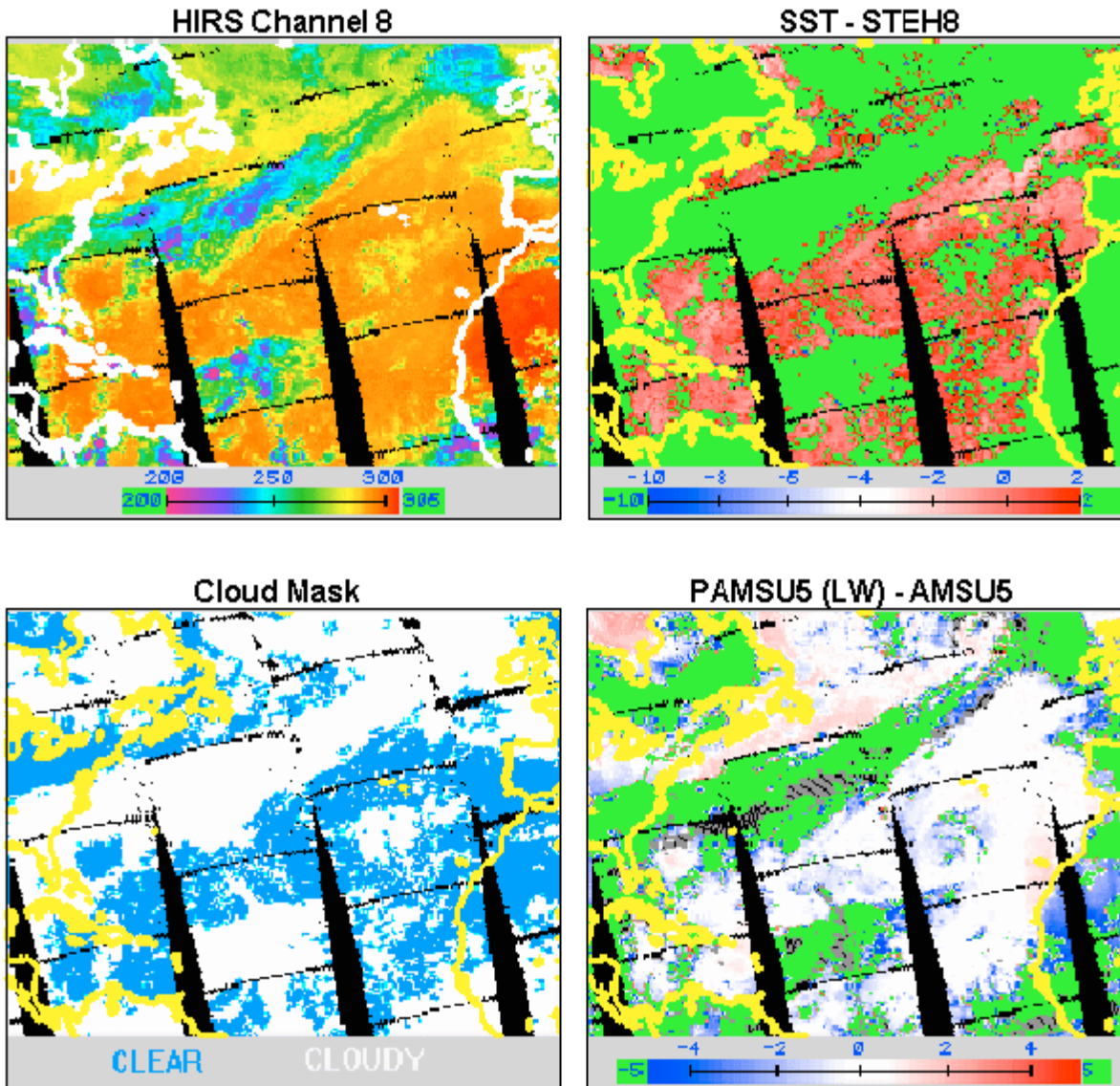


Figure 3: HIRS channel 8 radiance temperature ($^{\circ}\text{K}$) measurements (upper left), the corresponding cloud test differences (K) for “SST - STEH18” (upper right) and “PAMSU5 (LW) - AMSU5” (lower right) tests as defined in Table 1, and the resulting cloud mask (lower left), composited from 18Z on September 6 to 01Z on September 7, 2000 for NOAA-15.

3.1.4 First Guess

The first guess is uniquely determined for each ATOVS-A and ATOVS-B sounding using a library search technique (Goldberg et al. 1988). The first guess libraries consist of approximately 4000 collocations of radiosonde and satellite observations, which are directly accessed during orbital processing and updated daily. Separate libraries are maintained for the ATOVS-A and ATOVS-B systems, respectively, and for the clear and cloudy sounding collocations in ATOVS-A, respectively. The collocations within each library are also sorted based on terrain and latitude. First guess library compilation and updating is described in Section 3.2.2.4

The first guess (and retrieval) sequence for ATOVS-A is done for one HIRS fov, selected per 2x2 array across the scan. The overall selection hierarchy is clear, sea, non-sea¹² (except coast), and cloudy, meaning that clear/sea soundings have the highest priority, followed by clear/nonsea, cloudy/sea, and cloudy/nonsea. It is also required that at least 2 of the 4 candidates be designated as clear to derive a clear sounding, and sea to derive a sea sounding, respectively. If all 4 fov are designated the same, the fov with the warmest HIRS channel 8 value is selected¹³.

The first guess (and retrieval) sequence for ATOVS-B products is done for every other AMSU-B fov across the scan, excluding precipitating fov.

The library search technique utilizes sounder channel measurements as discriminators for searching the respective libraries and determining the first guess. The channels used, referred to as the channel combination, are determined by the sounding type. The cloud and terrain designation of the selected HIRS fov defines the ATOVS-A sounding type, and the terrain designation the ATOVS-B sounding type.

Tables 3 and 4 list the first guess (FG) channel combinations (CC) for ATOVS-A and ATOVS-B sounding types, respectively. Special procedures are deployed to not use HIRS channels when processing ATOVS-A soundings over high terrain (1500 m), and in high southern latitudes. This is required due to the small number of clear collocations from these regions.

The measurements used to search the libraries are the limb adjusted radiance temperatures for ATOVS-A, and the limb and radiance bias adjusted radiance temperatures for AMSU-B.

The matrix equation for the library search is given in (1):

$$D = (R - R_k)^t B^{-1} (R - R_k) \quad (1)$$

where the subscript t indicates the matrix transpose, -1 the inverse, and

- D : scalar closeness parameter,
- B : sounding channel radiance covariance matrix; dimension (35 x 35) or (5 x 5),
- R : adjusted, observed radiance temperature vector; channels FG (CC), and
- R_k : adjusted, library radiance temperature vector; channels FG (CC).

¹² The Nonsea sounding type includes land, coast, sea-ice, snow cover and high terrain.

¹³ If HIRS data are not available, a default location is selected.

The dimensions “35” and “5” for the B matrix in Equation (1) denote the total number of sounder channels available for the ATOVS-A (20 for HIRS plus 15 for AMSU-A) and ATOVS-B systems, respectively; not all are used (see Tables 3 and 4). The channels FG (CC) are those compared in the search to compute “D”, which depend on the sounding type consistent with Tables 3 and 4. The subscript “k” is the number of library collocations searched, typically about 1500 collocations per sounding type. The channel combination CC, the collocations searched, “k”, and B matrix all vary consistent with the sounding type.

The first guess temperature, moisture and radiance temperature profiles for a given sounding are computed by averaging the 10 closest collocations; that is, those with the smallest “D”. Radiosonde averages are used for temperature and moisture, and the adjusted measurements from the sounder are averaged for radiance temperature. As discussed later in Section 3.2.2.4, the radiosonde reports stored in first guess libraries must have originally been complete from at least 950 to 50 mb, and are extended downward to 1000 mb, and upward to 0.1 mb as required.

Sounding Type	Channel Combination (CC)	First Guess FG (CC)	Retrieval RE (CC)
Clear, Sea	1	HIRS 7, 10-12 AMSU-A 1, 4-14	HIRS 2-7,10,12,14-16 AMSU-A 4-14
Clear, Non-Sea	2	HIRS 7, 10-12 AMSU-A 5-14	HIRS 2-7,10 12,4-16 AMSU-A 5-14
Cloudy, Sea	3	AMSU-A 1, 5-14	AMSU-A 5-14
Cloudy, Non-Sea	4	AMSU-A 5-14	AMSU-A 5-14
High Terrain: > 1500 m	5	AMSU-A 5-14	AMSU-A 6-14
> 2500 m	6	AMSU-A 5,14	AMSU-A 7-14

Table 3: First Guess (FG) and Retrieval (RE) Channel Combinations (CC) for ATOVS-A Sounding Types.

Sounding Type	Channel Combination (CC)	First Guess FG (CC)	Retrieval RE (CC)
Sea	7	AMSU-B 1-5	AMSU-B 1-5
Non-Sea	8	AMSU-B 3-5	AMSU-B 3-5
Ice and >1500 m	9	AMSU-B 3-5	None

Table 4: First Guess (FG) and Retrieval (RE) Channel Combinations (CC) for ATOVS-B Sounding Types

The panels of Figure 4 show color-enhanced, composite fields of observed and first guess data across the northern and tropical Atlantic region, illustrating the first guess sequence for one channel and level. The sequence begins in the upper left panel with the sounder measurements, in this case AMSU channel 6 which is sensitive near 500 mb. The corresponding first guess measurement and 500 mb temperature fields are shown in the upper and lower right panels. Black regions indicate orbit gaps, with grey areas edited due to AMSU contamination (see Figure 2). Good consistency is observed between the first guess temperature and radiance temperature data, an important characteristic of the library search approach and pre-requisite for accurate retrievals (Fleming et al. 1986). Comparison to the concurrent cloud data shown in Figure 3 indicates that distinctions between clear and cloudy soundings are not evident in the guess.

3.1.5 Retrieval

The general form of the retrieval equation is given by (2):

$$T - T_g = C (R - R_g) \quad (2)$$

where T and R are product and measurement parameters, the subscript “g” an a priori estimate, and C is the solution.

The ATOVS-A retrieval method is the Minimum-Variance-Simultaneous (MVS) solution (Smith et al. 1984 and Fleming et al. 1986) given by matrix equation (3):

$$\begin{aligned} T - T_g &= S A^t (A S A^t + N)^{-1} (R - R_g) \\ &= X (Y)^{-1} (R - R_g) \end{aligned} \quad (3)$$

where the subscript *t* indicates the matrix transpose, -1 the inverse, and:

- T: final soundings products vector, (133),
- T_g: first guess products vector, (133)
- S: first guess covariance matrix, (133 x 133),
- A: sounder channel weighting matrix, (35 x 133),
- N: measurement noise covariance matrix, (35 x 35),
- R: observed radiance temperature vector, channels RE (CC),
- R_g: first guess radiance temperature vector, channels RE (CC), and
- X, Y: pre-computed retrieval operator components.

The product vector (T) contains 100 levels of atmospheric temperature (1000 mb to .1 mb), 32 levels of moisture (1000 mb to 200 mb), and the surface level¹⁴. The dimension 35 for the A and N matrices denotes all the ATOVS channels; not all are used. The channels RE (CC) denotes the first guess¹⁵ and observed channels used in the retrieval solution, depending on the sounding type consistent with Table 3.

¹⁴ The 100 levels of temperature and 32 levels of moisture are internal only.

¹⁵ The first guess observations for a given channel are available independent of whether they were used in the first guess search.

NOAA-15

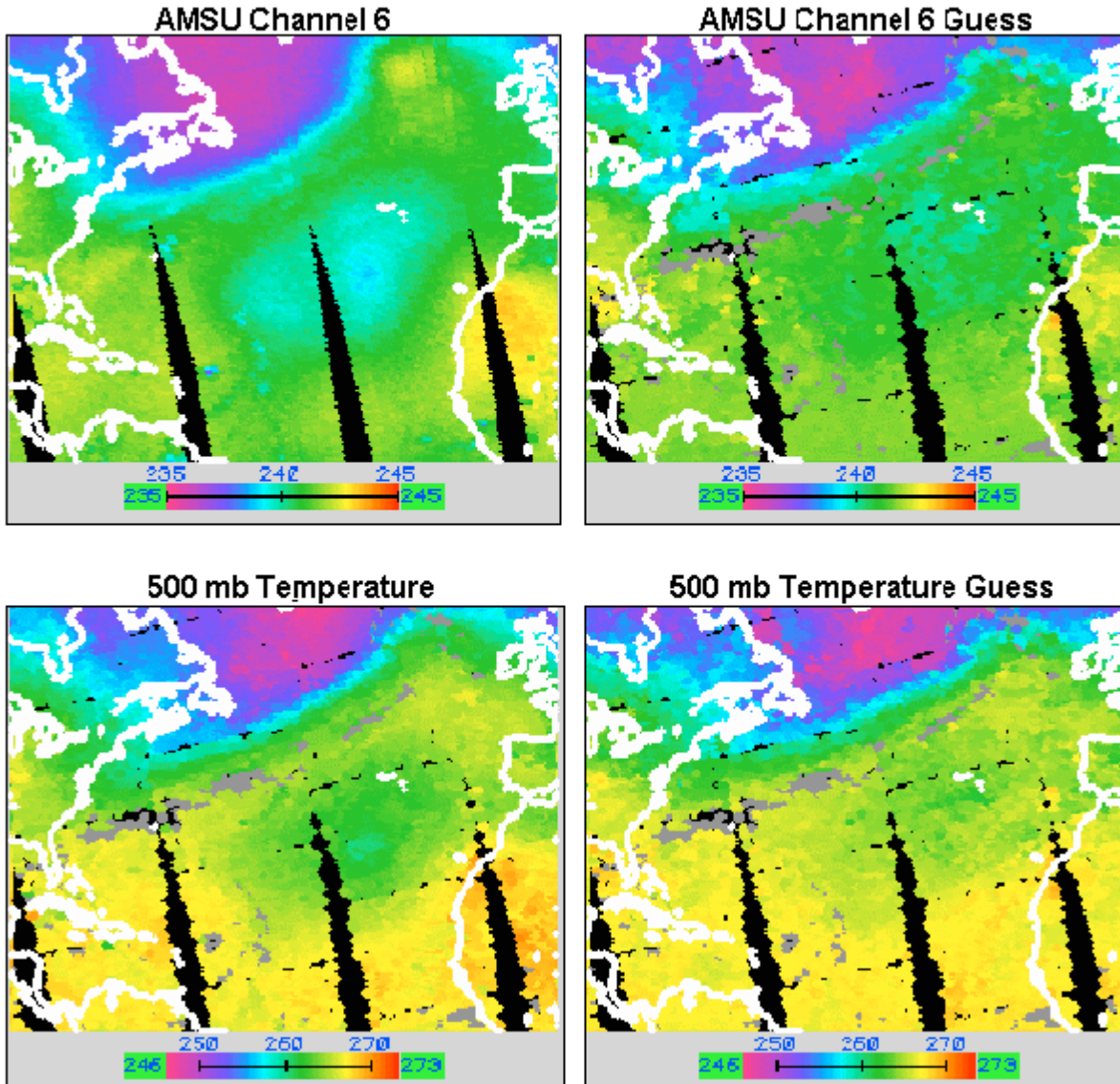


Figure 4: The first guess and retrieval sequence for one channel and level, showing AMSU-A channel 6 radiance temperature measurements ($^{\circ}$ K) (upper left), corresponding first guess measurements (upper right) and 500 mb temperatures (lower right) ($^{\circ}$ K), and 500 mb final sounding temperatures ($^{\circ}$ K) at 500 mb, composited from 18Z on September 6, to 01Z on September 7, 2000.

The X and Y components of the MVS retrieval operator are pre-computed offline and updated weekly. Thirty-two (32) sets of components are computed and selected for a given sounding based on the latitude, terrain type, and cloud designation. The calculation of the retrieval operators is described in Section 3.2.3.4.

The lower left panel of Figure 4 shows the retrieved temperature field at 500 mb, the final step in the first guess and retrieval sequence.

The ATOVS-B retrieval utilizes an ordinary least squares solution of equation 2, where:

- T: water vapor mixing ratio sounding products vector (15),
- T_g : first guess mixing ratio vector, (15),
- C: statistical regression coefficients (15 x RE (CC)),
- R: observed radiance temperature vector, channels RE (CC), and
- R_g : first guess radiance temperature vector, channels RE (CC).

The product vector (T) includes 15 levels of atmospheric moisture (1000 to 300 mb). The channels RE (CC) denote the AMSU-B channels used to compute the regression coefficients and derive sounding products. The channels used depend on the sounding type consistent with Table 4.

Two sets of regression coefficients are available, for sea and non-sea soundings respectively. Their calculation is addressed in Section 3.2.3.5.

3.1.6 Distribution

ATOVS-A operational sounding products are distributed to users at the conclusion of orbital processing, which takes about 20 minutes, with a complete orbit spanning 104 minutes.

The operational products that are routinely distributed to users include

- the original calibrated sounder measurements
- adjusted sounder measurements
- first guess information
- derived temperature and moisture soundings
- appended ancillary data (i.e., cloud mask, AVHRR, SST, etc.)

Dedicated links for these data include:

- NOAA-EMC
- United Kingdom Meteorological Office (UKMO, Bracknell, England)
- Global Telecommunications System (GTS)
- Shared Processing Network (SPN)¹⁶

The characteristics of the data provided over the various links include the level-1b data (Goodrum et al. 2000) and full density operational sounding products over the NOAA-EMC and

¹⁶ Files are placed into the SPN format and transmitted over the SPN, a dedicated link to the U.S. Navy and Air Force in support of operational NWP.

UKMO links, the full density operational products over the SPN, and a lower density product at an approximately 250 km spacing over the GTS.

ATOVS-B operational sounding products were only being distributed over the SPN.

The complete set of NESDIS operation sounding products is archived at NCDC (Goodrum et al. 2000).

3.2 OFFLINE PROCESSING

The Offline sub-systems (see Figure 1) comprise a significant portion of the sounding products system. Offline systems contribute the tuning and validation functions required to maintain the scientific integrity of the orbital sounding products.

Offline systems routinely compile and maintain data sets comprised of:

- Satellite Radiance Data Sets
- Satellite and Radiosonde Collocations
- Coefficients

3.2.1 Satellite Radiance Data Sets

Satellite Radiance Data Sets are separately maintained for HIRS/3, AMSU-A and AMSU-B radiometer data. These data sets contain about 100,000 observations of adjusted and non-adjusted (original) radiance temperature measurements at the respective instrument fov, typically spanning the latest 30 to 60 days. Each data set is updated at the conclusion of orbital processing at about a 10% sub-sampling rate, excluding polar-redundant and high terrain (>1500 m) observations.

Since the satellite Radiance Data Sets are compiled at the conclusion of orbital processing, they can include additional processed data. For example, HIRS/3 data records include interpolated AMSU-A measurements, the 17 concurrent AVHRR measurements, and are segregated based on the clear and cloudy designation. The AMSU-A (and AMSU-B) records include CLW amount and Precipitation edits (Figure 2).

The use of Satellite Radiance Data Sets to generate coefficients for orbital processing are described in Section 3.2.3.

3.2.2 Satellite and Radiosonde Collocations

Collocated radiosonde and satellite observations are extensively used in the derivation and validation of the operational sounding products. Their use to derive soundings, referred to as tuning (Reale et al. 1990), is described in the following sections. Their use in validation is presented in Section 4.1

Tuning provides routine compensations to reconcile systematic errors among the scientific algorithms, for example, the radiative transfer model (Uddstrom et al. 1994a and 1994b), the limb-adjusted (Wark 1993) satellite measurements used to derive products, and ground truth

radiosondes (McMillin et al. 1988 and 1992), and is a pre-requisite for maintaining accurate sounding products.

The steps to compile and utilize collocated radiosonde and satellite observations include:

- Radiosonde Processing
- Collocation Processing
- Matchup Data Base (MDB)
- First Guess Libraries

These four steps are updated daily.

3.2.2.1 Radiosonde Processing

Radiosonde reports received over the GTS are processed daily (Tilley et al. 2000). These reports are accessed from EMC holding files, include radiation correction (McMillin, et al. 1992), and range from eight to thirty-two hours old when processed by NESDIS, and must pass the following two sets of screening tests.

First, each report level is tested and designated as missing if:

- temperature data are missing or exceed climatological limits,
- dewpoint depression data are missing below 500 mb for temperatures $> -40^{\circ}$ C,
- dewpoint depression data exceed 50° C, or
- successive significant levels do not decrease in pressure

Radiosonde reports are then rejected if:

- any first significant level data are missing,
- the vertical extent for temperature does not reach 100 mb,
- the vertical extent for moisture does not reach 500 mb (for temperature $> -40^{\circ}$ C),
- there is an extensive gap (Tilley et al. 2000), or
- an excessive lapse rate (Tilley et al. 2000).

Accepted radiosonde reports are candidates for collocation with satellite data. Typically, about 1500 northern hemisphere and 200 southern hemisphere radiosonde reports are observed per day, and about 20% are rejected. Figure 5 shows a global distribution of accepted (o) and rejected (x) radiosondes from a single day.

3.2.2.2 Collocation Processing

A collocated radiosonde and satellite observation is compiled (Tilley et al. 2000) if the candidate radiosonde and satellite sounding data:

- are within specified time and distance windows,
- differ by less than 10° K for any temperature below 100 mb (ATOVS-A only), and
- have similar surface pressure

The time (t) and distance windows (x) for ATOVS-A are stratified per geographic category as defined in Table 5; for ATOVS-B the distance window is 100 km globally, and the time window is 3-hours for non-sea and 5-hours for sea soundings, respectively. Radiosonde versus satellite sounding temperature comparisons above which exceed 10° K at some level above 100 mb, result in a designation of missing data at and above that level. A surface pressure must be reported for a radiosonde, and must lie within one TOVS level of the satellite surface pressure (Reale et al. 1994).

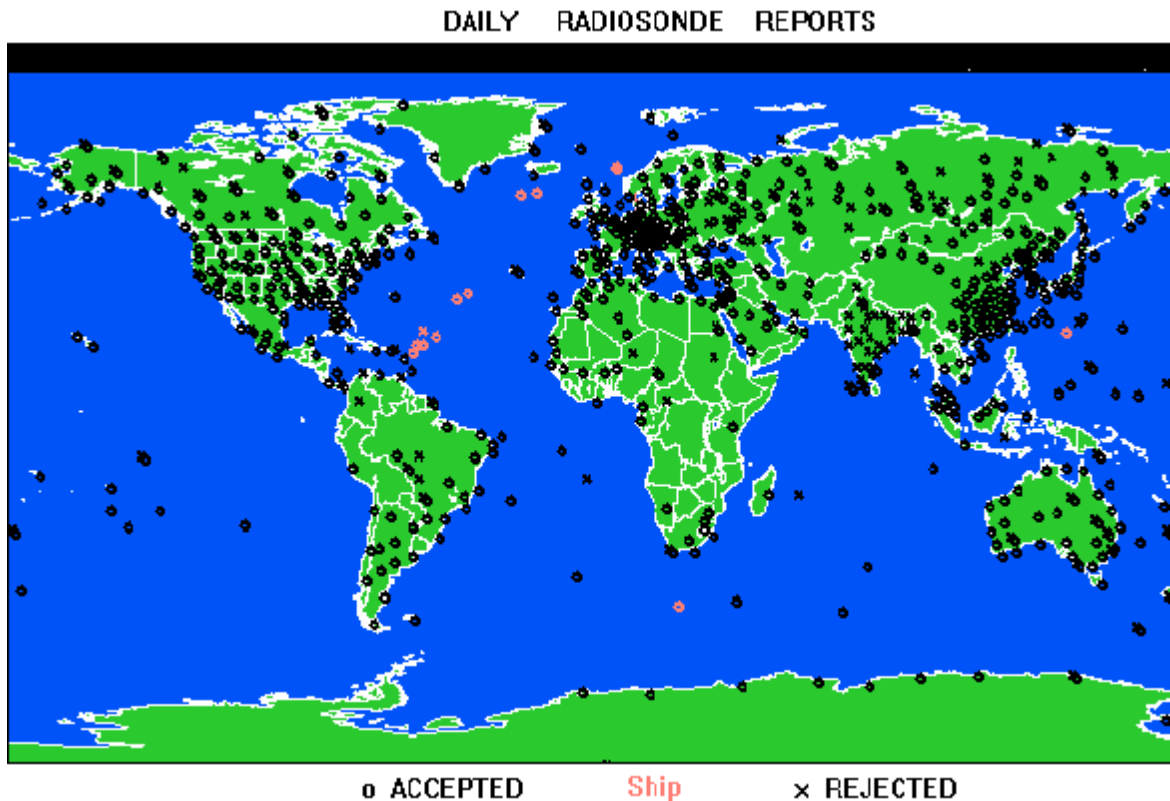


Figure 5: A typical global distribution of radiosonde reports from a single day.

Each radiosonde is limited to one collocation per satellite and sounding type, and a given sounding can only be collocated once. As discussed in Section 3.1, the sounding type is defined by the terrain of the sounding, namely sea or non-sea, and for ATOVS-A includes the clear or cloudy designation. Although the non-sea sounding type includes land, sea-ice, snow cover and coastal designations, only one is selected. Selected collocations are typically those closest in time, and then in space. The exceptions are coastal collocations, which are only selected if no other types are available¹⁷.

3.2.2.3 The Matchup Database (MDB)

The Matchup Data Base (MDB) supporting the ATOVS-A and ATOVS-B products systems, respectively, provides the longer term data sets of radiosonde and satellite data collocations used for the tuning and validation of derived sounding products (Tilley et al. 2000 and Reale et al. 1990). Each MDB is updated daily, with an approximately 80% overlap in sample from week to week.

The ATOVS-A system maintains separate MDB's for clear and cloudy collocations, each containing about 8,000 collocated radiosonde and satellite observations, which are stratified

¹⁷ Satellite measurements along coastlines are considered undesirable given the mixed sea and non-sea signatures across the fov (for example, for lower peaking microwave channels).

among 23 geographical categories. Each geographic category contains a target sample size, and sampling constraints which uniquely determine the spatial and temporal distribution of the collocations.

Table 5 lists the 23 categories (**CAT**) and associated criteria for the MDB in ATOVS-A. Each category is segregated by latitude belt (**LAT**) and terrain type (**TERR**), and the satellite orbit node (**Ascending**, **Descending** or **Both**). Each category contains separate distance (**x**) and time (**t**) windows, and target sample sizes (**Samp**) for the collocations stored, which are also listed, along with the typical time periods (**T**) spanned by the clear and cloudy collocations per category.

The MDB update procedure for ATOVS-A includes:

- independent sampling for each category,
- a chronological pre-sorting of the collocations per category within “500 km” spaced grid boxes, and
- sequential sampling of the most current observation within each grid box

Collocations are stored into each MDB category sequentially, depending upon their age in relation to a specified reference age. The reference age is initialized at 21-days, and increased (as necessary) in 7-day increments, up to 105 days, until the target sample size for a given category is met. This strategy provides a preferential retainment of more recent collocations from radiosonde dense regions (i.e., northern hemisphere), and older collocations from radiosonde sparse regions (i.e., southern hemisphere), thus maintaining a complimentary record of recent weather and complete global coverage.

The ATOVS-B system maintains a single MDB of about 15,000 collocated radiosonde and satellite observations stratified by sea and non-sea collocations, respectively.

The MDB for ATOVS-B is updated independently for sea and non-sea collocations respectively, and does not include much of the sampling strategies employed in ATOVS-A. The final sample of collocations tend to be heavily weighted toward northern hemisphere population centers, with a global sampling period of about 21 days. As discussed later in Section 5, a merged ATOVS-A and B system is planned which would inherit the ATOVS-A sampling strategies for MDB compilation.

The MDB for ATOVS-A is routinely archived by NCDC (Goodrum et al. 2000).

3.2.2.4 The First Guess Libraries

The First Guess Libraries are updated daily based on the MDB, and directly accessed during orbital processing. The first guess libraries have about half of the capacity of the MDB, with an additional requirement that the vertical extent of a candidate radiosonde report be complete from (at least) 950 mb to 50 mb for ATOVS-A, and from 950 mb to 400 mb for ATOVS-B, respectively.

There are two separate first guess libraries in ATOVS-A, corresponding to clear and cloudy collocations, respectively, and a single library containing all collocations in ATOVS-B. Each library contains about 5000 collocations segregated into sea and non-sea sections, and are updated daily consistent with the order in which they were stored onto the MDB. The right columns of Table 3 indicate the sample sizes per geographic category, and the associated time

CAT	Lat	Terr	Node	x (km)	t (hr)	Samp	MDB		Samp	Library	
							T-clear (days)	T-cldy (days)		T-clear (days)	T-cldy (days)
1 ¹⁸	N	Ice/C	B	100	3	350	50	30	200	30	21
2 ¹⁹	Ice-45N	Sea	B	60	4	650	30	25	350	21	20
3	45-30N	Sea	B	70	4	650	45	30	350	30	21
4	30-15N	Sea	B	80	4	600	55	35	350	35	21
5 ²⁰	15N-15S	All	B	60	4	650	30	30	350	21	21
6	15-30S	Sea	B	100	5	250	30	40	175	21	25
7	30-45S	Sea	B	100	5	250	30	30	175	21	21
8	45S-Ice	All	B	100	4	225	35	30	150	21	21
9	S	Ice/C	B	100	4	225	—	35	125	—	25
10	90-60N	Non-Sea	A	100	2	250	40	30	150	30	21
11	60-45N	Non-Sea	A	60	2	400	25	21	225	20	15
12	45-30N	Non-Sea	A	50	2	500	21	21	275	15	15
13	30-15N	Non-Sea	A	70	3	450	30	25	250	21	20
14	15-30S	Non-Sea	A	100	3	300	25	30	175	20	21
15	30-45S	Non-Sea	A	100	3	200	25	35	150	20	25
16	60-90S	Non-Sea	A	100	3	25	—	100	15	—	100
17	90-60N	Non-Sea	D	100	2	250	30	25	150	21	20
18	60-45N	Non-Sea	D	60	2	400	25	21	225	20	15
19	45-30N	Non-Sea	D	50	2	500	21	21	275	15	15
20	30-15N	Non-Sea	D	80	3	400	50	25	225	30	20
21	15-30S	Non-Sea	D	100	3	250	35	70	150	21	40
22	30-45S	Non-Sea	D	100	3	200	35	35	150	21	21
23	60-90S	Non-Sea	D	100	3	25	—	100	15	—	100
Total	Sample					8000			4650		

Table 5: The 23 categories (CAT) and associated sampling criteria and characteristics for the MDB and First Guess Libraries of ATOVS-A on September 6, 2000

periods spanned by the clear and cloudy collocations stored on the first guess libraries for ATOVS-A.

Figure 6 illustrates a typical global distribution of collocations stored on the first guess libraries for combined clear and cloudy collocations from NOAA-15. The sounding location is used for plotting, and the color coding for the collocated sounding is sea (light blue), land (dark green), coast (yellow), ice (grey) and snow (white). Collocations with ship radiosondes are red.

The compilation of first guess libraries for ATOVS-A includes an upward extrapolation of each radiosonde temperature profile from the highest report level (i.e., at least 50 mb) to .1 mb, and a downward extrapolation (if necessary) to 1000 mb.

¹⁸ Includes Northern Hemisphere Ice, and 60N to 90N coastal, collocations.

¹⁹ Includes Sea collocations from the Ice-edge to 45N.

²⁰ Includes Sea and Non-sea collocations.

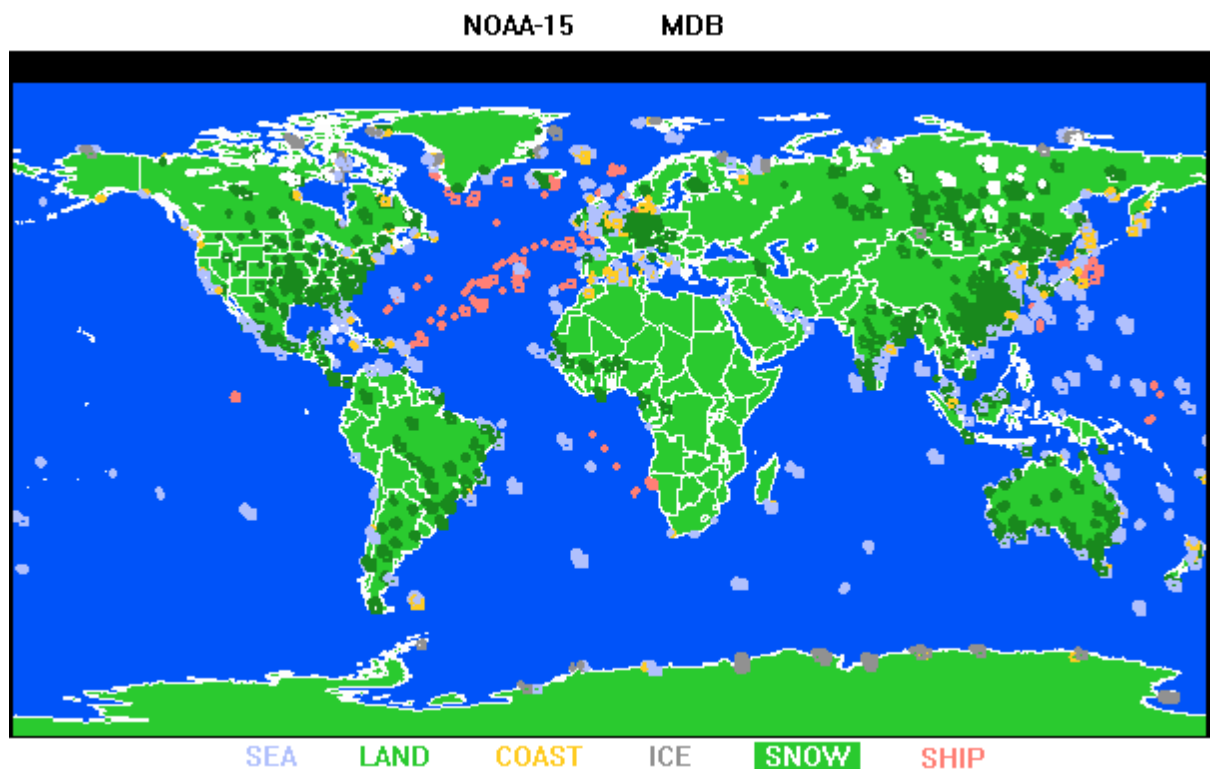


Figure 6: The global distribution of clear and cloudy collocations stored on the First Guess Libraries from NOAA-15 observed on September 6, 2000.

A new approach based on a statistical regression of the collocated AMSU-A measurements (Goldberg 1999) was deployed for NOAA-15 during April 2000 to extend each radiosonde from the highest report level to .1 mb. A requirement for extension is that the difference between the regressed and observed radiosonde temperature profiles must be within 2.5 degrees at some level between 10 mb and 60 mb. The level at which the absolute difference is minimum is defined as the merge point, with values as and above this level provided by the regression, and below provided by the radiosonde. If no merge point is found, the collocation is not stored in the library. Typically, less than ten (10) percent of the candidate collocations fail these criteria.

The downward extension of radiosonde is only required if the first significant level was between 950 and 1000 mb, and is done using a weighted, averaged, lapse rate and constant dewpoint depression for temperature and moisture, respectively, based on the lowest reported levels.

Reported and extrapolated radiosonde profile data as described above are stored in the first guess library, and directly available during orbital processing to determine the first guess (Section 3.1.4).

3.2.3 Coefficients

Coefficients for the derivation of operational sounding products are required for

- Limb Adjustment,
- Cloud Detection,
- First Guess,
- Retrieval,
- Radiance Bias Adjustment (AMSU-B only), and
- RFI Correction (AMSU-B for NOAA-15)

Except for limb adjustment, all coefficients are updated weekly.

3.2.3.1 Limb Adjustment

Regression coefficients for limb adjusting the HIRS/3, AMSU-A and AMSU-B (Wark 1993) are computed from the respective Satellite Radiance Data sets. Coefficients are independent for each sounder, based solely on the calibrated, radiance temperature, measurements, and include smoothing constraints across the scan. Three “associated” channels are normally used when applying corrections, the channel itself and those peaking immediately above and below²¹. Associated channels are constrained to not mix temperature, moisture and surface sensitivity measurements.

Separate sets of limb correction coefficients are generated for sea and non-sea observations, respectively. In the absence of significant instrument drift, an initial set of coefficients can last for the operational life-span of the satellite, typically two to three years²². NESDIS maintains operational monitoring of scan position residuals for all sounders and channels, and updates coefficients as necessary (Allegrino et al. 1999).

3.2.3.2 Cloud Detection

Coefficients for the regression based, cloud detection tests for ATOVS-A (see Table 1) are updated weekly using the HIRS Satellite Radiance Data set, and an ordinary least squares regression. Limb adjusted and cloud-free measurements are used, with the AMSU-A measurements interpolated to the HIRS field-of-view (fov), and the 17 AVHRR centered on the HIRS fov (Ferguson and Reale 2000). No measurements poleward of 80 degrees latitude or for terrain heights greater than 1000 m are used.

Table 6 lists the predictands, predictors, parameter names (see Table 1) and sampling constraints for each set of coefficients. The sample sizes typically used to generate these coefficients are on the order of 50,000 observations, spanning the most recent 30 to 50 days.

3.2.3.3 First Guess

The radiance covariance “B” matrices (Goldberg et al. 1989) for the library search (see equation 1) are computed using the satellite measurements stored on the MDB. B-matrices are based on

²¹ Except in the case of surface and tropopause channels.

²² An exception are the limb adjustment coefficients for NOAA-15 which must be updated concurrent with RFI correction tables (see Appendix B).

adjusted radiance temperature observations consistent with those used in the library search and retrieval steps for each system, respectively, and consistent with the sounding type.

Four (4) “B” matrices are available in ATOVS-A, derived from clear and cloudy measurements, respectively, over sea and non-sea terrains, respectively.

Two (2) “B” matrices are available for ATOVS-B, derived from sea and non-sea measurements, respectively.

3.2.3.4 ATOVS-A Retrieval

The retrieval operator components (“X” and “Y” of equation 3) for ATOVS-A temperature and moisture soundings are updated weekly using the collocations stored on the MDB, with vertical extent requirements and extrapolation for radiosonde similar to the first guess libraries. As indicated in Equation 3, the retrieval operator components consist of the:

- A-matrix providing sounding channel weights for each retrieval level,
- the S-matrix providing the vertical covariance of first guess (or background) error, and
- the N-matrix providing the sounder measurement uncertainty.

Internal matrix calculations are all scaled to 700 cm^{-1} ²³.

Predictand	Predictors	Parameter	Constraint
SST	HIRS 6, 7, 10, 11, 8	STEH 8	DAY, SEA
SST	HIRS 6, 7, 10, 11, 18	STEH 18	NIGHT, SEA
SST	HIRS 6, 7, 10, 11, 19	STEH 19	NIGHT, SEA
AVHRR 3	AVHRR 4	PAVHRR 3	NIGHT, SNOW AND ICE FREE
AVHRR 4	AVHRR 5	PAVHRR 4	NONE
HIRS 7	HIRS 13-16	PHIRS 7	NIGHT
AMSU-A 5	HIRS 13 -16	PAMSU5 (SW)	NIGHT
AMSU-A 5	HIRS 4 - 7	PAMSU5 (LW)	NONE
AMSU-A 7	HIRS 13 -16	PAMSU7 (SW)	NIGHT
AMSU-A 7	HIRS 4 - 7	PAMSU7 (LW)	NONE

Table 6. Predictand, predictor(s), parameter name and sampling constraints for regression coefficients used in cloud detection.

²³ Measurements are converted to 700 cm^{-1} equivalent radiance as originally required to utilize the pre-computed S matrices from Crosby et al. (1973).

Nine (9) “A” matrices provide the vertical weighting function (Fleming et al. 1986) curves for each ATOVS sounding channel. Each matrix is computed based on combined samples of clear and cloudy collocations as stored in the MDB geographical categories 1 through 9, respectively (see Table 5). Individual and mean profiles of the satellite measurements and radiosonde (temperature and moisture) data, and corresponding atmospheric transmittance profiles (McMillin et al. 1995) are used to compute an A-matrix for each collocation, which are then averaged over the category to compute the A-Matrices available for retrieval.

The three (3) differential (d) terms comprising each A-matrix element for a given microwave sounding channel, CM, and pressure level, P, reduces to (4):

$$(CM, P) = (dR(700) / dB T) \square (dT(P) / dR(700)) \square d\tau(P) \quad (4)$$

where,

- R(700) is the scaled equivalent Radiance at 700 cm⁻¹,
- BT is the channel Brightness Temperature (°K),
- T is the radiosonde Temperature (°K), and
- Tau is atmospheric Transmittance.

Term 1 is computed in the vicinity of the observed sounder channel measurements (BT), whereas terms 2 and 3 are relative to the radiosonde temperature (T) and transmittance (Tau) profiles in the vicinity of level (P). The corresponding terms for HIRS channels are more complex given their nonlinear relationship to temperature.

Figure 7 shows examples of the mean temperature (solid, thick curves) profiles for MDB categories 1 (blue) and 5 (red), representing polar and tropical atmospheres, respectively, and the corresponding A-matrix (or vertical weighting function) profiles for HIRS/3, channel 7 (dashed curves), followed by AMSU-A channels 5, 8, and 13 (thin, solid curves). The set of blue weighting curves correspond to the polar profile, and the red curves the tropical profile. The vertical axis indicates the geopotential height (km), the upper horizontal axis indicates atmospheric temperature (°K), and the lower horizontal axis the weighting function values (from equation 4). The date of these profiles was from September, 2000.

It can be seen that each channel is sensitive through a different atmospheric layer, and that the shape of each curve varies per atmosphere. Since the actual height (geopotential) of a given pressure level varies per atmosphere, plotting the weighting function curves in this manner accentuates their variation with height on a global scale, and as approximated through the nine “A” matrices. As discussed in Section 5, future plans include the use of unique A-matrix per sounding based on the first guess.

Noteworthy are the HIRS channel 7 curves, which illustrate their relatively high vertical resolution and sensitivity in the lower troposphere compared to AMSU, particularly in the Tropics.

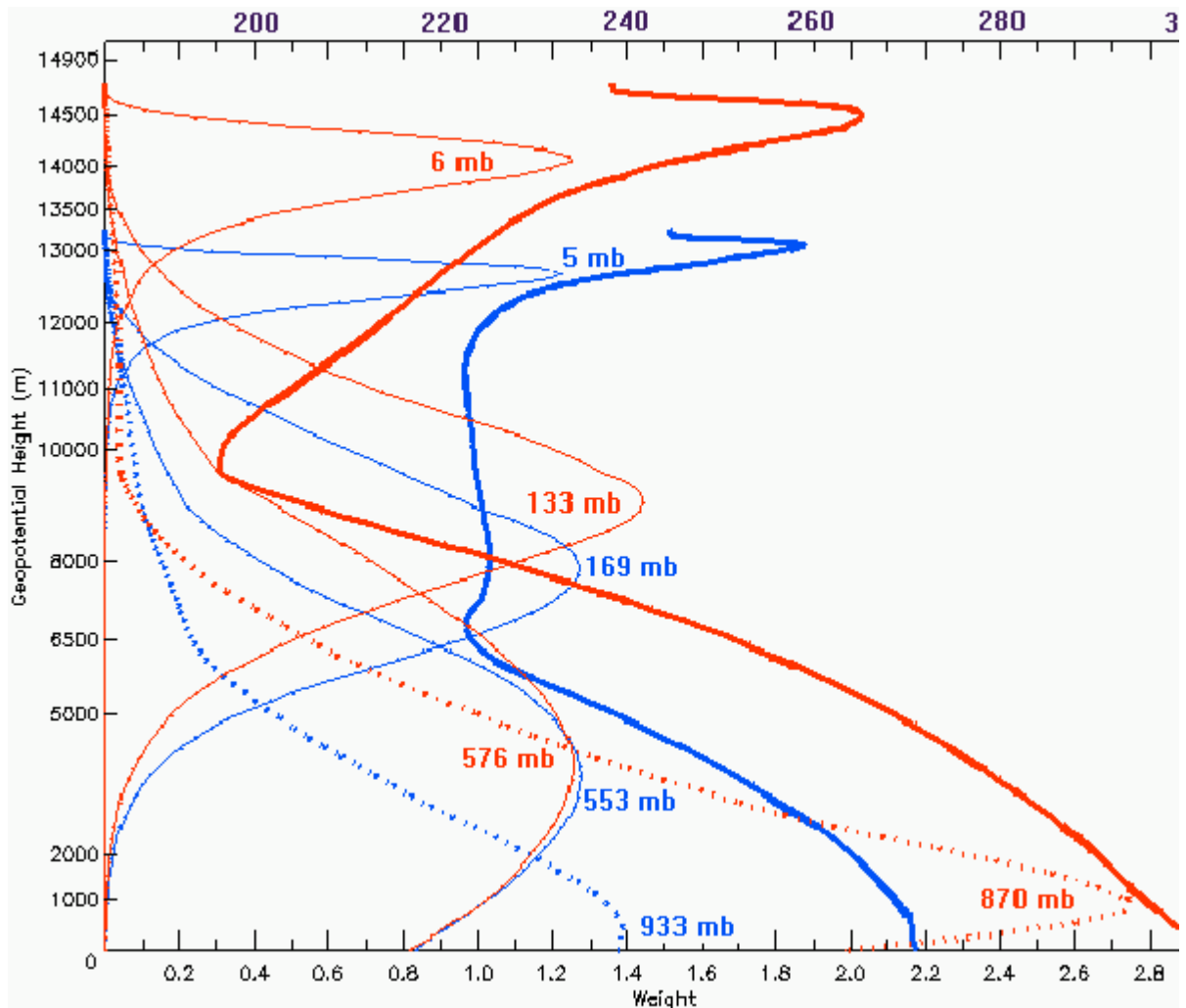


Figure 7: Mean temperature profiles ($^{\circ}\text{K}$) for Polar (solid blue) and Tropical (solid red) atmospheres, overlaid by corresponding weighting function curves for HIRS/3 channel 7 (dashed), and (in ascending order) by AMSU-A channels 5, 8 and 13 for NOAA-16, as computed for the Polar (blue) and Tropical (red) atmospheres versus geopotential height (m) (vertical axis), with the temperature ($^{\circ}\text{K}$) and weight values defined along the upper and lower horizontal axis.

Four (4) “S” matrices (Fleming et al. 1986) are computed which contain the vertical covariance of the “first guess minus radiosonde” differences for temperature and moisture at each pressure level. Separate matrices are computed based on the respective samples of clear and cloudy collocations for sea and non-sea terrains as stored on the MDB (see Table 5).

The S-matrix used to derive a given sounding is designed to be consistent with the collocations searched to determine the first guess, which as discussed earlier depends on the sounding type. These matrices constrain the retrieval solution based on the expected vertical correlation of the first guess minus sounding differences for temperature and moisture, including cross correlations between temperature, moisture and surface terms.

The “N” matrix is tri-diagonal and contains the noise equivalent in radiance (Fleming et al. 1986) for each channel, based on observed sounder calibration data (from the satellite). The final noise values depend upon temperature, and are uniquely computed using the mean profiles for MDB geographical categories 1 through 9, respectively (see table 5).

Thirty-two (32) total sets of retrieval operator components are computed using specific combinations of the nine (9) A-matrices, and four (4) S-matrices as described above. Seven (7) operators are available for sea soundings, and nine (9) are available for nonsea soundings, with separate sets of operators for clear and cloudy sounding types. The retrieval operator and channel combination used, that is, the specific operator components and the rows and columns of the A and N matrices for a given sounding, is defined by the sounding type and geographic category consistent with Tables 3 and 5²⁴.

3.2.3.5 ATOVS-B Retrieval

The retrieval coefficients for AMSU-B moisture soundings are computed using the collocations stored on the MDB and an ordinary least-squares regression solution (Crone et al. 1996). The radiosondes used must satisfy the vertical extent requirements and require extrapolation similar to the first guess libraries (for moisture and temperature)

Radiosonde minus first guess water vapor mixing ratios are regressed against the observed minus first guess radiance temperature values. The radiance temperatures used are both limb and bias adjusted.

Two sets of global regression coefficients are computed from sea and non-sea collocations (Goldberg et al. 1998), respectively, consistent with the channel combinations in Table 4.

3.2.3.6 Radiance Bias (AMSU-B)

Radiance temperature bias adjustment coefficients (Fleming et al. 1991 and McMillin et al. 1989) for AMSU-B are computed using a shrinkage-estimator, constrained, regression approach (Crone et al. 1996). Coefficients are based on radiance temperatures calculated (McMillin et al. 1995) from the radiosondes, versus the collocated, limb-adjusted measurements as stored on the MDB. The CLW (Grody et al. 1999) is included as a predictor for radiance bias adjustments over sea.

²⁴ Retrieval operators for corresponding, ascending and descending categories over non-sea terrains are identical.

Two sets of global regression coefficients are computed based on sea and non-sea collocations, respectively.

Figure 8 illustrates an example of the magnitude and global characteristics of the radiance bias adjustments. The upper panel shows bias adjusted radiance temperature measurements for the AMSU-B 183 ± 1 GHz channel, which is sensitive to upper tropospheric moisture, and the lower panel the magnitude of the bias adjustments applied. As can be seen, the adjustments for this channel are on the order of 5 degrees K, with a tendency for positive adjustments in the southern hemisphere than in the north, perhaps indicative of a seasonal trend. Adjustments over land tend to be negative, and slightly larger than over sea.

Overall, the bias adjustments appear to enhance the measurement field patterns, an encouraging aspect, but the large magnitude of the adjustments is troublesome, suggesting significant error in either the radiative transfer model or radiosondes, the latter particularly suspect concerning upper tropospheric moisture (Soden et al. 1996).

Upon updating the radiance bias coefficients, all the bias adjusted observations stored on the MDB are re-calculated. This is done prior to the weekly updating of the first guess libraries, radiance temperature covariance matrices and retrieval regression coefficients to maintain consistency between expected and measured observations during the upcoming week.

3.2.3.7 RFI Correction Tables

As discussed in Appendix-B, the RFI correction tables for AMSU-B onboard NOAA-15 require periodic adjustment (Atkinson 2000). This requires subsequent actions to re-calculate the

- limb adjustment coefficients,
- limb adjusted observations on the MDB,
- bias adjustment coefficients,
- bias adjusted observations on the MDB,
- radiance covariance “B” matrices, and
- retrieval regression coefficients.

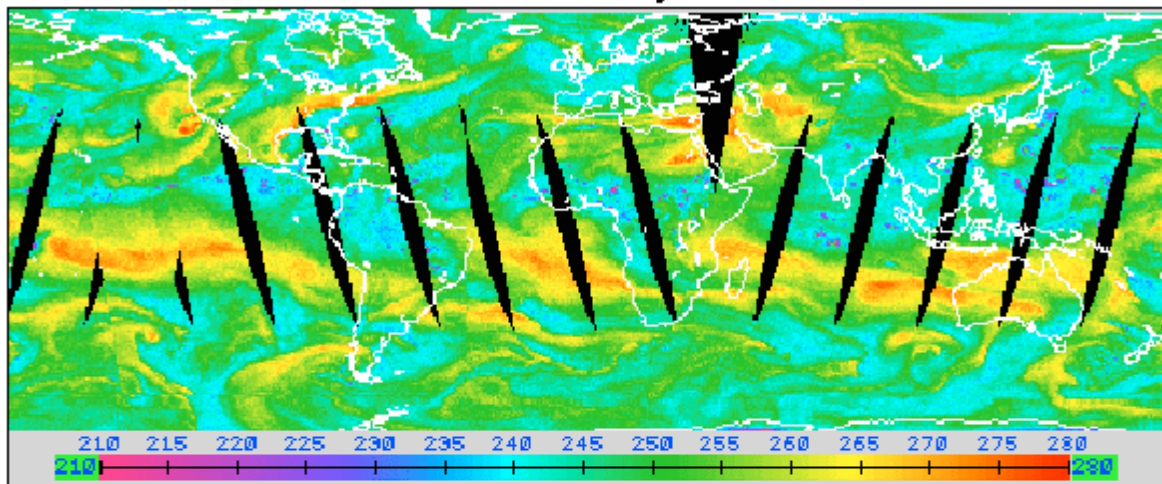
These are provided as required.

4 RESULTS AND ANALYSIS

The scientific monitoring and evaluation of operational sounding products is maintained on a continuous basis at NESDIS. The primary validation strategies consist of

- vertical accuracy statistics and
- horizontal field analysis

NOAA-15 AMSU-B 183 +/- 1 GHz
Radiance Bias Adjusted



Bias Adjustment

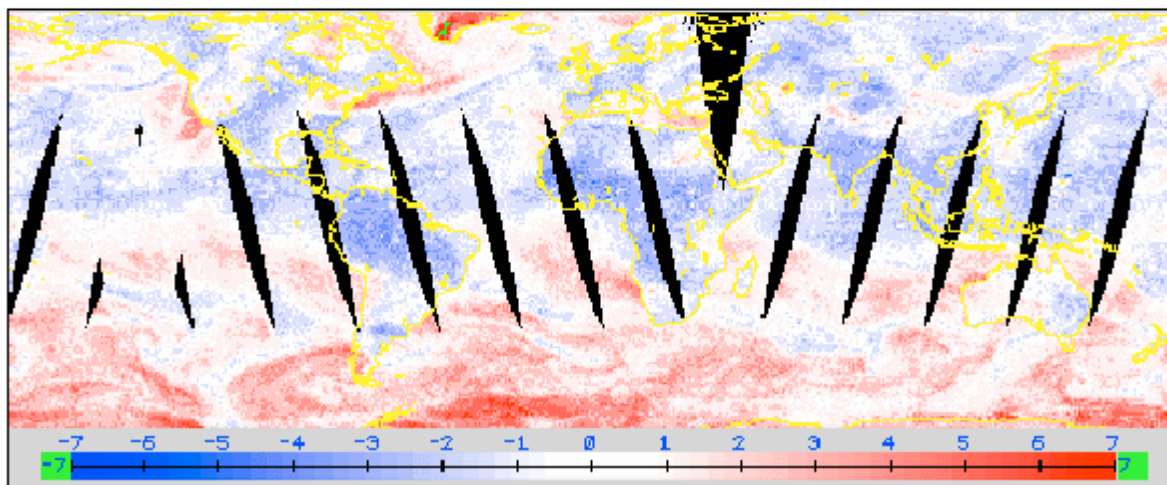


Figure 8: Bias adjusted radiance temperature measurements ($^{\circ}\text{K}$) for the AMSU-B upper tropospheric moisture channel at $183 \pm 1 \text{ GHz}$, onboard NOAA-15, and the corresponding magnitude of adjustments (lower), composited from 16Z on September 6 to 05Z on September 7, 2000.

4.1 Vertical Accuracy Statistics

Vertical accuracy statistics based on satellite minus radiosondes differences computed from collocations stored on the MDB are illustrated in Figures 9 and 10, which provide estimates of the expected performance of NESDIS operational soundings on a global scale. Figure 9 shows differences for ATOVS-A clear (left) and cloudy (right) temperature soundings, respectively, from the 60N to 60S latitude belt. Figure 10 shows differences for ATOVS-B moisture soundings for the 90N to 30N and 30N to 30S latitude belts, respectively. The thicker curves for each plot are for the final soundings, and the thinner lines for the corresponding first guess profiles, respectively. Figure 9 provides mean and standard deviation differences in degrees K, whereas the Figure 10 plots are percent differences in water vapor mixing ratio (g/kg), with the mean profiles used to compute percentages shown along the inside of the left axis. Pressure (mb) and sample size are indicated along the left and right vertical axis for all plots.

Figure 9 indicates that uncertainties for the clear and cloudy temperature soundings are comparable, with satellite minus radiosonde differences approaching 2.5° K Root Mean Square (RMS) near the surface and troposphere, 1.5° K in the middle troposphere where the sounders are most reliable, and about 2.0° K in the stratosphere. Clear soundings appear to be slightly more accurate than cloudy soundings near the surface, and both sets show little or no bias except at the tropopause.

Figure 10 indicates expected uncertainties for moisture near the surface to range from 15 percent in the tropics to 25 percent in polar regions. However, when multiplied by the mean mixing ratio values, the actual differences in water mixing ratio units is about 2 g/kg in the Tropics, versus 1 g/kg outside the tropics. Similarly, the steady increase in the percentage uncertainty of moisture with height is also attributable to the relatively low mixing ratio values aloft. Factoring in the spatial and temporal windows for each collocation, the inherent variability of moisture measurements, and radiosonde moisture errors (Schmidlin 1998, Soden et al. 1996, and Wang et al. 2001), the accuracy estimates shown in Figure 10 are reasonable.

Another feature of these statistics is the convergent aspect of the retrieval solution for ATOVS-A, manifested in Figure 9 through the significantly improved accuracy of the final soundings (thick curves) compared to the guess (thin curves). This confirms the scientific approach, in particular, the consistency of the first guess radiance temperature and temperature observations provided for the retrieval step (Fleming et al. 1986).

4.2 Horizontal Fields

Horizontal field analysis provides better meteorological context concerning the characteristics of the derived satellite products than the vertical accuracy statistics, and is an important component of the product validation function at NESDIS. Such analysis allows comparisons of sequentially composite fields of sounder measurements and associated derived products data, and as available concurrent NWP fields. Figures 11 through 15 illustrate examples of meteorological analysis over regional and synoptic scales, for various atmospheric levels and satellite data types. All are concurrent with the 16 Z to 05Z time frame spanning September 6 and 7, 2000, similar to other horizontal fields presented in this report.

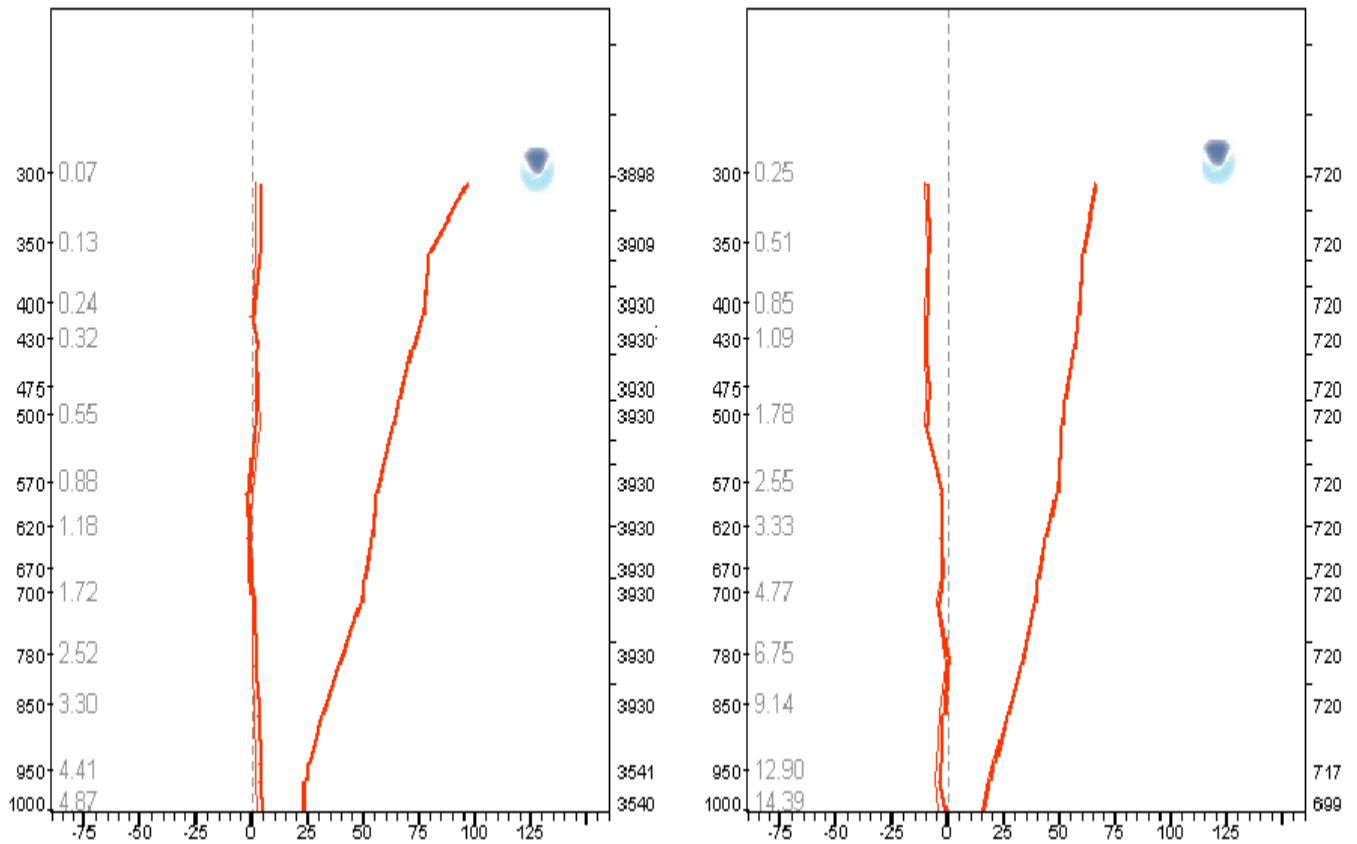


Figure 10: Satellite minus radiosonde mean and standard deviation differences (%) for ATOVS-B first guess (thin) and final (thick) moisture soundings from the 90N to 30N (left) and 30N to 30S regions, respectively, during a 7-day period in September, 2000. Differences are percentages of the mean mixing ratio profiles (g/kg) shown on the inside of the left axis, with pressure on the outer left axis and sample size on the right axis.

The four panels of Figure 11 illustrate regional scale analysis for a storm system in the N. Atlantic as it approaches northern Europe. The two upper panels display AMSU measurements for channel 6, sensitive in the middle troposphere, versus satellite minus NWP difference fields for the 500 mb to 300 mb layer-mean, virtual temperature. The two lower panels show AMSU channel 5, sensitive in the lower troposphere, and satellite minus NWP differences for 1000 mb to 700 mb layer mean virtual temperature. The NWP are from the EMC Aviation Forecast cycle (Caplan et al 1997) and are the 6-hour forecast valid within ± 3 hours of the satellite observation time (as appended during Preprocessing). Color scales are shown below each plot; for difference fields, white indicates values within $\pm 1^\circ$ K. The composite time period for each field is approximately 18Z to 22Z.

Analysis of Figure 11 indicates that differences between the satellite and NWP data are in regions of strong temperature advection (Reale 1995c). Agreement elsewhere is quite good (i.e., white), including in the warm and cold air cores. These differences also appear to be correlated with the prevailing advection pattern, with positive (red) values in areas of warm advection, and negative (blue) values in areas of cold advection²⁵. The vertical structure of the differences is also meteorologically consistent, for example, the area of positive values (warm advection) aloft (upper right panel) lie well east of the area of positive values closer to the surface (lower right panel).

The four panels of Figure 12 illustrate satellite based upper tropospheric structures concurrent with Figure 11. Shown are the AMSU-A channels 8 (upper left) and 7 (lower left), with peak sensitivities which on the average lie just below and above the tropopause, around 250 mb and 150 mb, respectively (see Appendix-A1 and Table 8). The corresponding right panels show derived temperature sounding fields at 250 and 150 mb, respectively.

Figure 12 shows good agreement between the sounder measurement and derived temperature patterns. Particularly interesting is the anomalous warm region in the AMSU channel 7 and associated 250 mb temperatures fields. This feature signifies a region of minimum tropopause heights, and maximum tropopause level change, typically associated with a developing upper air low pressure trough and located just north of the jet stream-stream core. Combined with the analysis of AMSU channel 8, both the jet stream and level of maximum wind are indicated just below the line at which the tropopause cuts the 200 mb surface (Wickham 1970).

The three panels of Figure 13 show NOAA/EMC analysis fields (Caplan et al.1997) for 250 mb temperature (upper), tropopause pressure (middle), and 250 mb wind (lower), averaged over a 12-hour period beginning at 00Z on September 7, about 6 hours later than the satellite data. Except for the slight (expected) eastward shift, the EMC analysis supports the satellite analysis in Figure 12. AMSU-A radiance measurements are directly assimilated into EMC NWP forecasts (Derber et al. 1998), which accounts for the good agreement between the satellite and EMC data in this otherwise data devoid region.

²⁵ Not attributable to time differences between the satellite and NWP valid times (Reale 1995c).

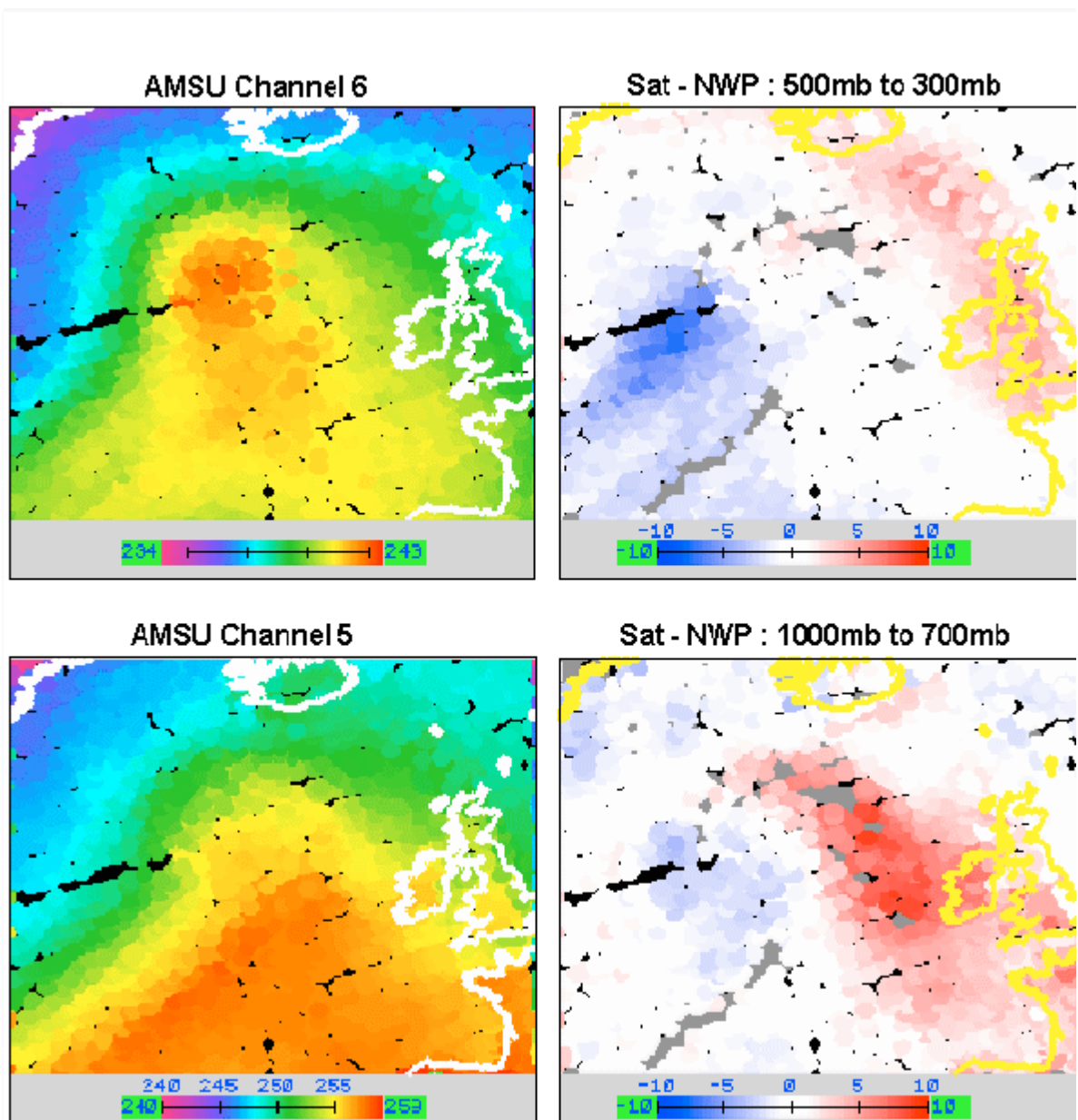


Figure 11: AMSU-A radiance temperature measurements ($^{\circ}$ K) for channels 6 and 5, and corresponding Satellite minus NWP forecast difference ($^{\circ}$ K) fields for upper (500 to 300 mb) and lower (1000 to 700 mb) tropospheric layers, respectively, composited from 18Z to 22Z on September 6, 2000 for NOAA-15.

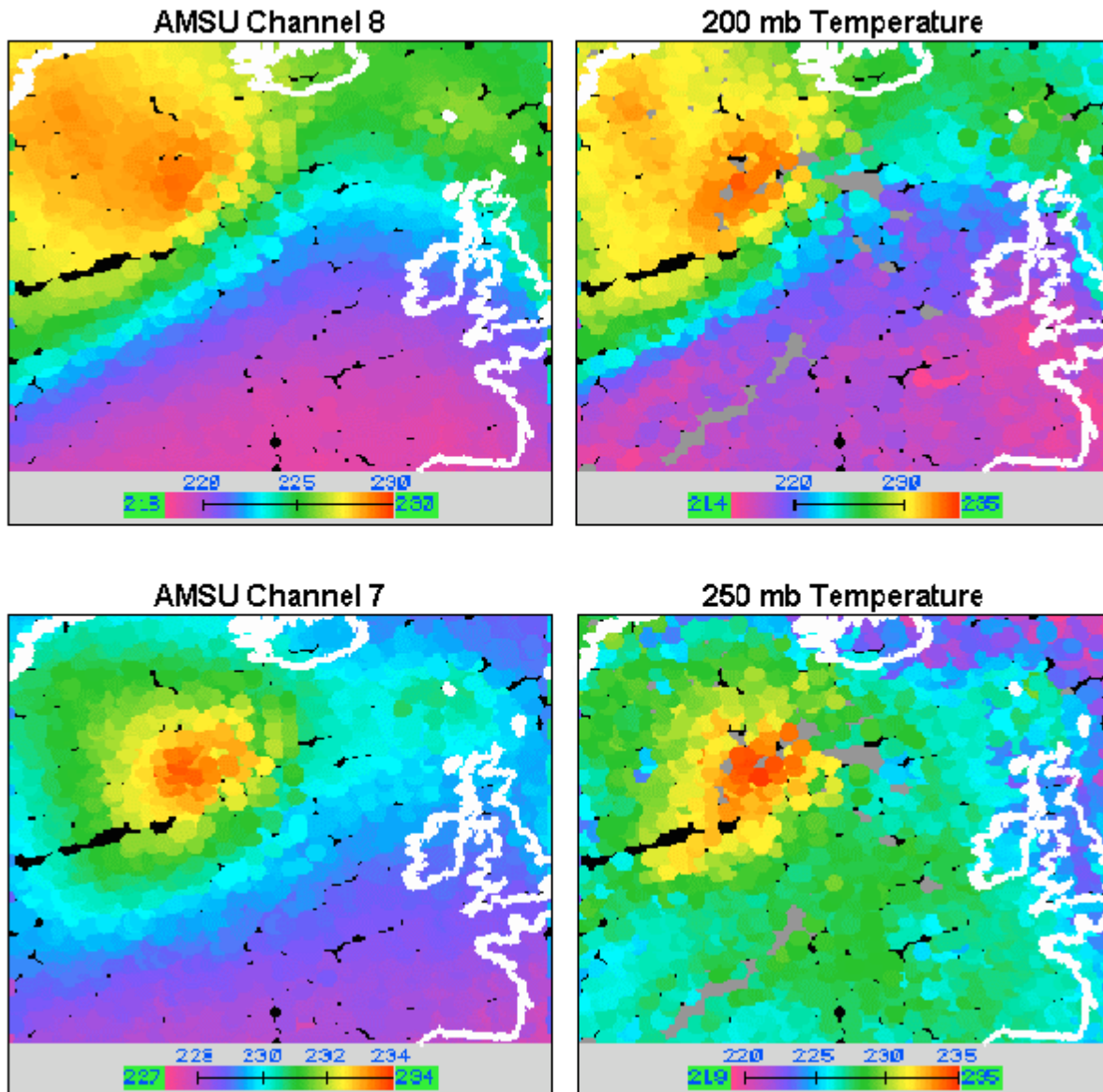


Figure 12: AMSU-A radiance temperature measurements ($^{\circ}$ K) for channels 7 and 8, and corresponding satellite sounding temperature fields ($^{\circ}$ K) at 250 and 200 mb, composited from 18Z to 22Z on September 6, 2000, for NOAA-15.

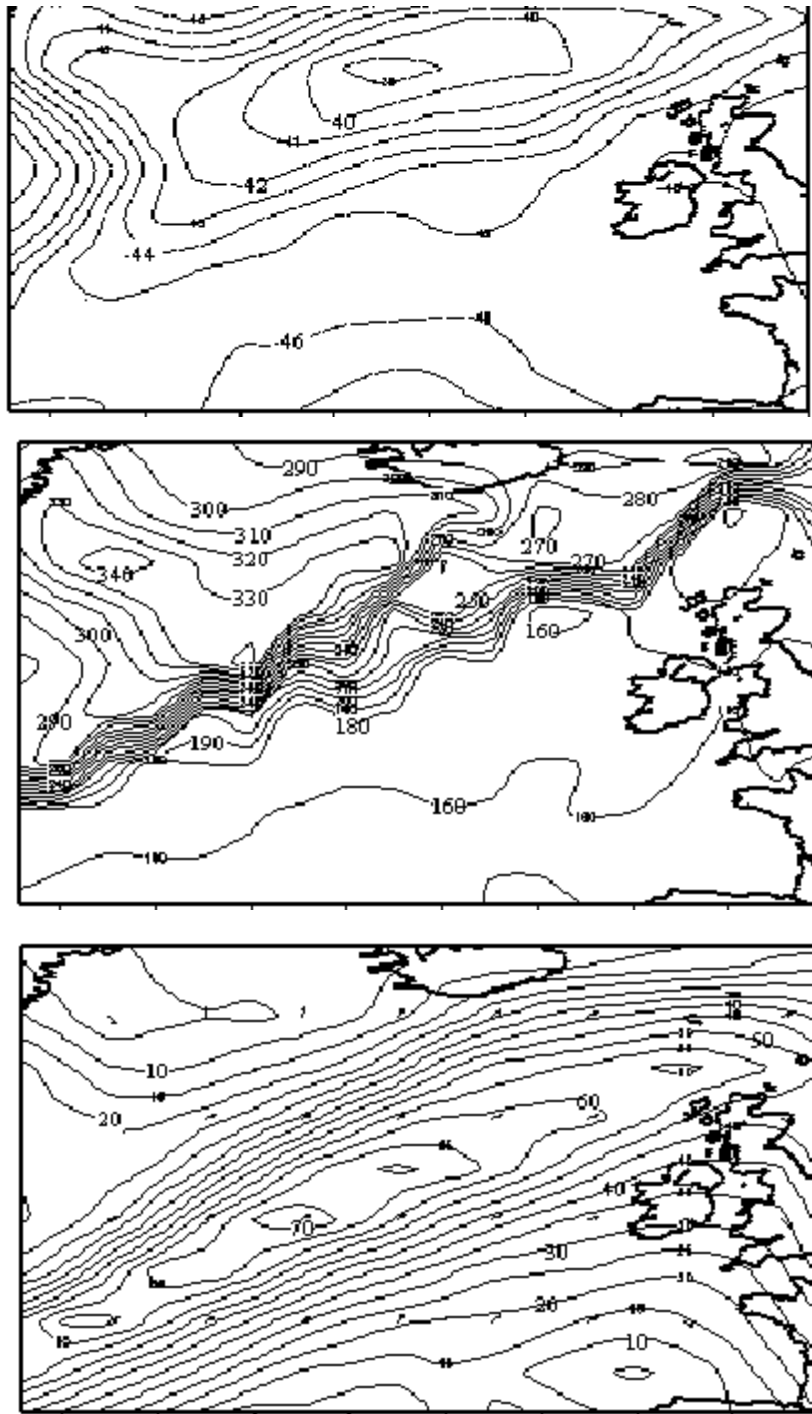


Figure 13: EMC 12-hour averaged fields for analyzed 250 mb temperature °C (upper), tropopause pressure (mb) (middle), and 250 mb winds (knots) (lower) for 06Z on September 7, 2000.

The four panels of Figure 14 provide satellite based cloud and moisture data for this case. The HIRS channel 8 (sensitive to cloud) and experimental cloud-top pressure²⁶ (Yang et al 1996) data in the upper left and right panels illustrate the cloud features for the region. Particularly interesting is the circular cloud structure in the HIRS 8 and cloud products, which appear to outline the surface low. Combined with the satellite data shown in Figures 11 and 12, the zonal plane of a developing baroclinic wave (Wallace and Hobbs 1977) is portrayed. The vertical, westward tilt of the wave trough is denoted by a curve from the surface low, westward, through the AMSU channel 6 and 7 warm cores, with the trough at 200 mb situated over the cold air at lower levels. Maximum cold advection and subsidence in the middle troposphere are typically observed south and west of this line, with maximum warm advection and lifting to the north and east. System intensification is probable, consistent with the analysis of the satellite minus NWP differences from Figure 11.

The lower panels of Figure 14 illustrate the corresponding AMSU-B, mid-tropospheric, moisture data. Again noticeable is the circular cloud feature, but this time in the AMSU-B 183 ± 3 GHz measurements (lower left) reputedly transparent to clouds. This channel also shows warming (dryness) associated with the “warm core” in AMSU-A channel 7 (Figure 12), as would be expected in a subsiding cold air mass. Also evident is a dry zone to the east of the surface low, indicative of residual subsidence from the previous system. The derived AMSU-B moisture field at 620 mb is shown in the lower right panel. Overall consistency is seen between the AMSU-B measurements and derived products, although contamination consistent with the infra-red cloud signature is also evident.

The four panels of Figure 15 show expanded horizontal coverage of the AMSU-B moisture data for the upper troposphere. Each set of panels displays the AMSU-B 183 ± 1 GHz channel, sensitive to upper tropospheric moisture, and corresponding derived moisture products at 500 mb. The two upper panels provide an approximately 7-hour composite covering the northern hemisphere region, and concurrent with the CLW, precipitation, and cloud data shown earlier in Figures 2 and 3. The two lower panels span 12-hours, covering a larger region from Africa westward to the middle Pacific. Good consistency is observed among all these data, illustrating the robust patterns of upper level moisture measurements and derived products on a regional and global scale. Remote satellite products are a primary source of contiguous and reliable upper level moisture data.

Satellite derived products are also the primary source of global temperature data in the upper stratosphere (Finger et al. 1993). The four panels of Figure 16 illustrate 12-hour composite fields of global coverage for AMSU-A channel 13 adjusted radiance temperature measurements (upper left) which are sensitive in the vicinity of 5 mb (see Figure 8), corresponding 5 mb derived temperature fields from NOAA-15 (upper right) and from RTOVS for NOAA-14 (lower left), and the NOAA-15 minus NOAA-14 temperature differences at 5 mb (lower right). Color scales are indicated below each panel, with identical spectral scales used for the respective 5 mb temperature fields.

²⁶ Experimental ATOVS-A cloud products include cloud top pressure, cloud top temperature and cloud amount at HIRS fov.

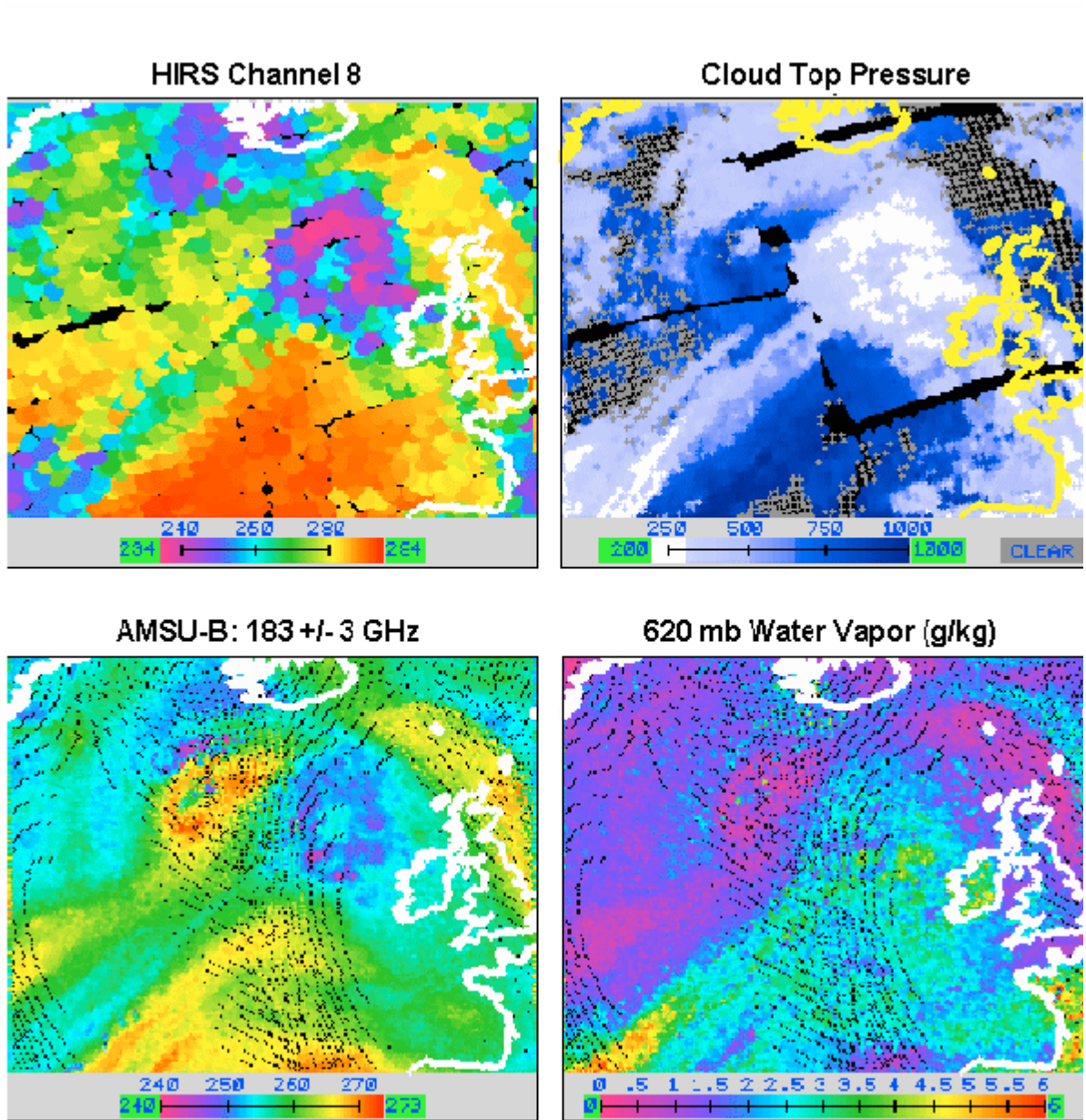


Figure 14: HIRS channel 8 radiance temperature ($^{\circ}$ K) measurements (upper left), derived cloud-top pressure (mb) (upper right), and concurrent AMSU-B radiance temperature measurements ($^{\circ}$ K) at 183 ± 3 GHz. (lower left) and derived moisture (g/kg) at 620 mb (lower right), composited from 18Z to 22Z on September 6, 2000 for NOAA-15.

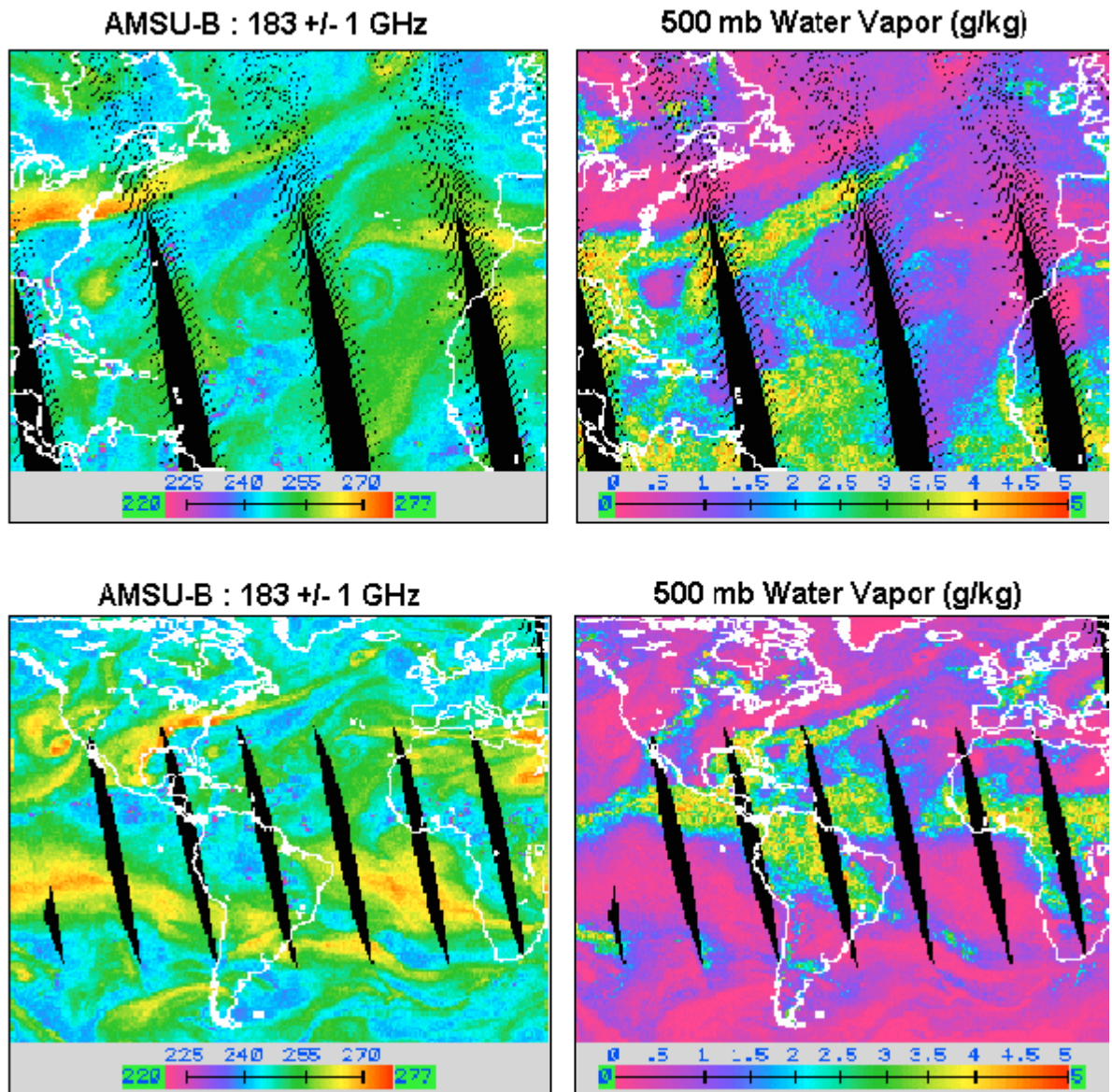


Figure 15: AMSU-B radiance temperature measurements ($^{\circ}$ K) at 183 ± 1 GHz. (left panels) and derived 500 mb moisture (g/kg) for composited fields from approximately 18Z to 0Z (upper), and 16 Z to 4Z (lower) on September 6 and 7, 2000 for NOAA-15.

As seen in Figure 16, the 5 mb temperature patterns for NOAA-15, ATOVS, are tightly aligned with the channel 13 measurements, and differ significantly with their NOAA-14 counterparts. Absolute differences between these satellites are on the order of 5° K over most of the Tropics, and exceed 10° K in south polar regions²⁷. This is attributable to the new ATOVS approach for upper stratospheric soundings discussed in Section 3.2.2.4. Comparisons against available Halogen Occultation Experiment (HALOE) soundings above 10 mb have been used to verify the improved performance of the ATOVS upper stratospheric products (Goldberg 1999).

5 FUTURE PLANS

The NESDIS operational system provides a dynamic research environment which includes an ongoing program to develop, evaluate and implement scientific (and system) upgrades for sounding products based on user feedback and internal monitoring.

The primary scientific activities planned over the next year is the merging of the ATOVS-A and B systems into a single, simultaneous, temperature and moisture products generation system. This will include studies to replace the library search with a statistical regression technique based on AMSU, and if successful, the replacement of pre-computed with real-time retrieval operators. Referred to as System-2002, the proposed upgrade would result in dual sounding products, consisting of climate oriented first guess information, and real-time weather oriented derived products, the later optimized for assimilation into NWP. There are also new requirements to provide ATOVS processing fall back contingencies, particularly in the event of a HIRS sounder failure.

Preliminary work on System-2002 has been completed to subsample the AMSU-B onto the AMSU-A (and HIRS), including averaging of the (nine) corresponding AMSU-B measurements²⁸. Preliminary design of the regression guess and accompanying physical retrieval solution is underway. A significant component of these changes entails an increased use of radiative transfer calculations (McMillin, 1995) during orbital and offline processing. The plan includes fixed regression coefficients, based on calculated radiance from radiosondes (and rocketsondes), to compute the orbital guess products, followed by the calculation of associated first guess radiance²⁹. This would also require the radiance bias adjustment of the AMSU and HIRS/3³⁰ sounder measurements used in the retrieval step for consistency with the calculated first guess measurements. The requirement to calculate the first guess measurements also means that radiative transfer parameters required for the retrieval A-matrix would be uniquely available for each sounding, removing the need for pre-computed retrieval operators.

System-2002 will include a restructuring of the daily and weekly updating procedures. Although the daily compilation of collocated radiosonde and satellite data (onto the MDB) will continue, their application in products tuning will be modified and the first guess libraries discontinued. New radiosonde sampling methods are also anticipated, for example, options to screen the radiosondes used for tuning based on instrument type³¹ could significantly improve the global characteristics of derived product background errors from satellites.

²⁷ Vertical analysis also shows significant lapse rate differences as well in most global regions.

²⁸ Data sets retaining the original AMSU-B resolution would be available upon request.

²⁹ This was not necessary with the library search approach which provided averaged sounder measurements.

³⁰ The bias adjustment of HIRS has never been demonstrated operationally and presents unique problems due to clouds.

³¹ The Vaisala RS80 radiosonde is used at about 40 percent of the global operational radiosonde stations.

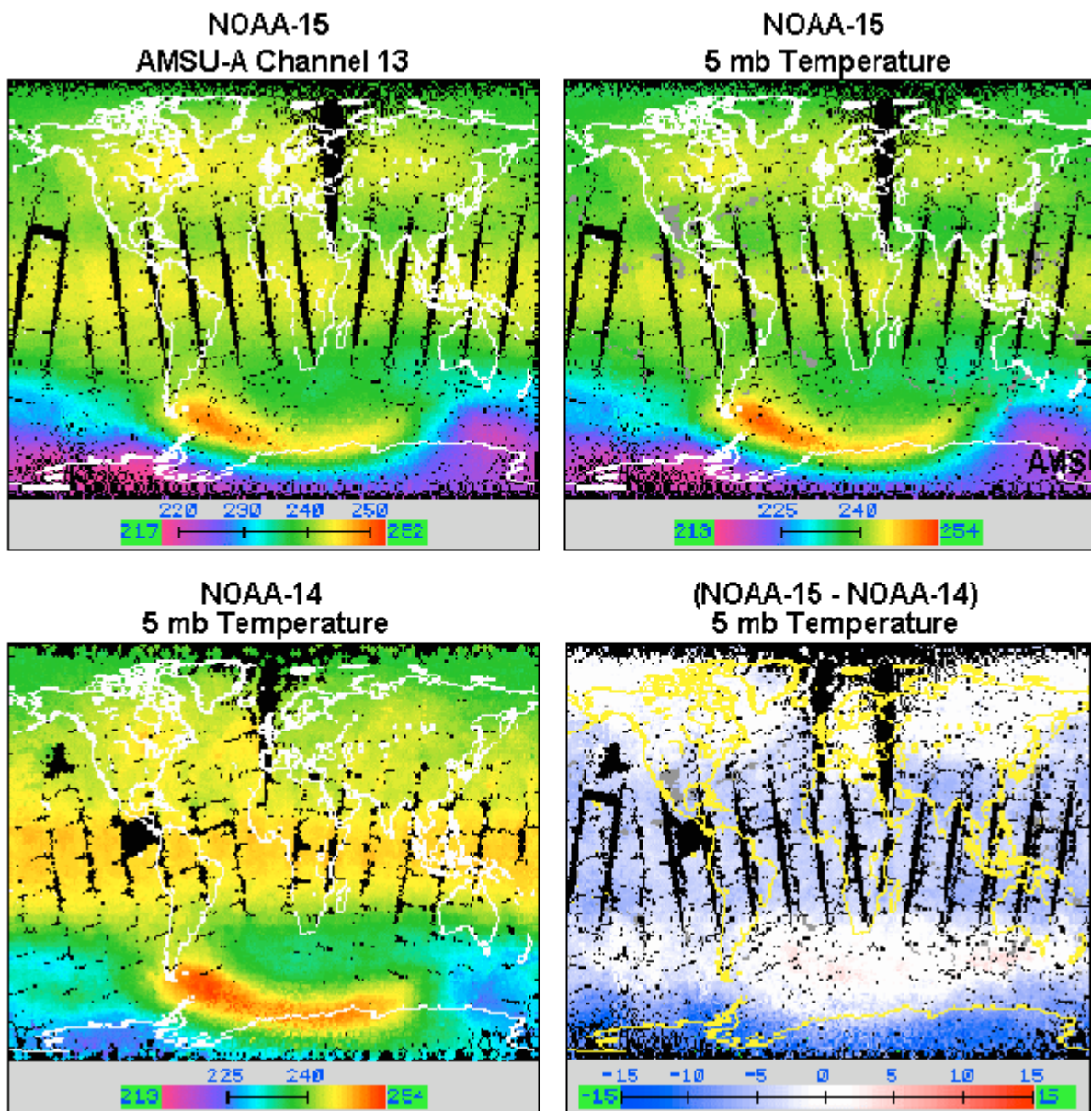


Figure 16: AMSU-A radiance temperature measurements ($^{\circ}\text{K}$) for channel 13 (upper left) and derived temperatures ($^{\circ}\text{K}$) at 5mb for NOAA-15 (upper right) and for NOAA-14 (lower left), and NOAA-15 minus NOAA-14 temperature difference at 5 mb, composited for the period 16 Z to 05Z on September 6 and 7, 2000.

6 SUMMARY

This report presents the current status of the NESDIS operational sounding products systems as of June, 2001. The report provides a brief history of the operational science algorithms since the onset of operational sounding products in 1979, leading up to the current ATOVS systems. ATOVS sounding products actually comprise two (2) separate systems, the ATOVS-A which processes AMSU-A, HIRS and AVHRR measurements to derive temperature and moisture sounding, and cloud products, and ATOVS-B which processes AMSU-B moisture sounding products. The processing systems for each are structured in a similar manner concerning Online (orbital) and Offline support systems.

Online (orbital) processing systems consist of a series of steps which screen the incoming sounder measurements, detect the presence of precipitation and cloud, compute first guess information, and derive sounding products. These steps are outlined with supporting graphical displays.

Offline support systems operate on a daily and weekly basis to provide data sets and coefficients which are used to derive the sounding products and for validation. These steps are outlined with supporting graphics.

Results are presented on the vertical accuracy and meteorological consistency of the derived sounding products. Statistical comparisons against collocated radiosondes provide estimates of derived sounding uncertainties on the order of 2.0 degrees RMS for temperature, and approaching 15 percent for low level moisture, with little or no bias. Meteorological case studies illustrate the horizontal and vertical consistency of the derived product fields across active weather systems on a regional and global scale. Both sets of results underscore the reliability of the NESDIS operational sounding products for global weather, as well as NWS field office applications.

The report concludes with a summary of future plans to merge AMSU-A and AMSU-B measurements (along with the infrared) in a proposed System-2002 configuration, which would provide separate sounding products for climate and weather applications, the latter optimized for NWP assimilation.

7 ACKNOWLEDGMENTS

I would like to thank Dr. Dieter Klaes (EUMETSAT), Dr. John Bates (NOAA), Mr. Michael Mignogno (NOAA) and Mr. Mitchell Goldberg (NOAA) for their thoughtful reviews of this report, and Ms. Joan Reed (NOAA) for final editing and preparation for publication. The work presented in the report would not have been possible without the continued support of my NOAA co-workers Mr. Michael Chalfant and Ms. Ellen Brown, and the contractor staff from Raytheon Corporation.

APPENDIX A1

AMSU-A RADIOMETER CHANNEL CHARACTERISTICS

Channel	Center Frequency (GHz)	Peak Sensitivity	Product
1	23.8	Surface	TPW, CLW
2	31.4	Surface	TPW, CLW
3	50.3	Surface	
4	50.8	850 mb	T
5	53.6	600 mb	T
6	54.4	400 mb	T
7	54.9	250 mb	T
8	55.5	150 mb	T
9	57.3	80 mb	T
10	57.3, $\pm .217$	50 mb	T
11	57.3, $\pm .322$ $\pm .048$	20 mb	T
12	57.3, $\pm .322$ $\pm .022$	10 mb	T
13	57.3, $\pm .322$ $\pm .010$	5 mb	T
14	57.3, $\pm .322$ $\pm .004$	2 mb	T
15	89.0	Surface	

TABLE A1

Table A1 shows the channel number, center frequency (GHz), the atmospheric pressure of peak sensitivity, and atmospheric product retrieved for each of the AMSU-A radiometer channels onboard NOAA-15. The two frequencies shown for channel 10 (i.e., $\pm .217$), and four frequencies shown for channels 11 to 14 correspond to the two and four pass bands done for the respective channels. The peak pressure sensitivities shown are based on calculations using the OPTRAN radiative transfer model (McMillin et al. 1995), and U.S. Standard Atmosphere (1976). The products shown correspond only to those derived during the operational processing of soundings.

APPENDIX A2

HIRS/3 RADIOMETER CHANNEL CHARACTERISTICS

Channel	Center Frequency (cm^{-1})	Peak Sensitivity	Product
1	669.1	25 mb	
2	678.8	50 mb	T
3	690.5	70 mb	T
4	703.1	250 mb	T, Cloud
5	715.9	400 mb	T, Cloud
6	731.7	600 mb	T, Cloud
7	747.7	900 mb	T, Cloud
8	897.4	Surface	Cloud
9	1032	30 mb	(O3)
10	801.1	Surface	H2O, Cloud
11	1362	500 mb	H2O, Cloud
12	1529	300 mb	H2O
13	2188	1000 mb	T, Cloud
14	2209	600 mb	T, Cloud
15	2235	350 mb	T, Cloud
16	2242	300 mb	T, Cloud
17	2419	Surface	
18	2518	Surface	Cloud
19	2657	Surface	Cloud
20	14,500 (.69 micron)	Visible	Cloud

TABLE A2

Table A2 shows the channel number, center frequency (cm^{-1}), the atmospheric pressure of peak sensitivity, and atmospheric product retrieved for each of the HIRS/3 radiometer channels onboard NOAA-15. The peak pressures are based on radiative calculations using OPTRAN (McMillin et al. 1995) and U.S. Standard Atmosphere (1976). Products correspond only to those derived during the operational processing of soundings; for Ozone (O3) products see Neuendorffer (1996).

APPENDIX A3

AVHRR RADIOMETER CHANNEL CHARACTERISTICS

Channel (micron)	Center Frequency	Peak Sensitivity	Product
1	.63	Visible	
2	.86	Visible	
3a	1.61	Visible	
3b	3.74	Surface	Cloud
4	10.8	Surface	Cloud
5	12.0	Surface	Cloud

TABLE A3a

AMSU-B RADIOMETER CHANNEL CHARACTERISTICS

Channel (GHz)	Center Frequency	Peak Sensitivity	Product
1	89	Surface	CLW
2	150	Surface	CLW
3	183 ± 1	350 mb	H2O
4	183 ± 3	500 mb	H2O
5	183 ± 7	650 mb	H2O

TABLE A3b

The above tables show the channel number, center frequency, the atmospheric pressure of peak sensitivity, and atmospheric product retrieved for each of the AVHRR radiometer channels (upper table), and AMSU-B radiometer channels (lower table) onboard NOAA-15. Center frequency is listed in microns for AVHRR, and GHz for AMSU-B. The two frequencies shown for AMSU-B channels 3 to 5 (i.e., ± 1, 3 and 7) correspond to the two (2) pass bands done for each channel. The peak pressure sensitivities (for AMSU-B) are based on calculations using the OPTRAN radiative transfer model (McMillin et al. 1995) and U.S. Standard Atmosphere (1976). The products shown correspond only to those derived during the operational processing of soundings.

APPENDIX B

RFI CORRECTION PROCEDURE

Preprocessing for ATOVS-B also includes the correction of AMSU-B measurements for Radio Frequency Interference (RFI) from data transmitters onboard NOAA-15 (Atkinson 2000 and Chalfant et al.1999); AMSU-B from NOAA-16 have no RFI.

The RFI correction procedures require three basic steps:

- determine which transmitters are on for a given scan line,
- correct the calibration points and compute “corrected” calibration coefficients,
- correct the earth views and apply corrected calibration coefficients.

Figure B1 shows horizontal imagery of color enhanced AMSU-B measurements and the impact of the RFI. The data are shown for AMSU-B channel 4 at 183 ± 3 GHz, sensitive to atmospheric moisture in the middle troposphere, and the channel most affected by RFI. The upper panel shows the original RFI contaminated data ($^{\circ}$ K), the middle panel the corrected AMSU-B data, and the lower panel the magnitude of the corrections applied ($^{\circ}$ K). The graphics were created special for illustrative purposes, since the actual RFI correction is done prior to the calibration step (which converts counts to radiance temperature) (Atkinson 1999).

Figure B1 illustrates the complex characteristics of the RFI, and its significant impact on the AMSU-B channel 4 measurements, up to 37° K in radiance temperature units.

Figure B2 shows plots of the RFI correction values across the scan for each AMSU-B channel, with the vertical axis showing the RFI correction in counts, and the horizontal axis each of the ninety-one AMSU-B scan positions. Each plot represents a different time period.

The upper panel of Figure B2 shows the original RFI values per scan position and channel from the S-band Transmitter (STX)-1 and STX-3, and the Search And Rescue Repeater (SARR) observed shortly after launch of NOAA-15 on May 13, 1998 (Atkinson 1999). A maximum RFI of about 1800 counts is observed for AMSU-B channel 2 (150 GHz).

The middle panel of Figure B2 shows the RFI correction values after September 28th, 1999, when NOAA turned off the STX-1 and STX-3 transmitters, leaving direct broadcast users reliant on STX-2 (which was not interfering with AMSU-B). The RFI correction values are significantly reduced for all channels, with a maximum value of about 600 counts for AMSU-B channel 4 (183 ± 3 GHz).

The levels of RFI affecting AMSU-B data are routinely monitored by NOAA and the United Kingdom Meteorological Office (UKMO), with the UKMO providing updated correction tables every 2 months along with recommendations to NOAA on whether the current correction tables need to be updated. The RFI correction pattern updated as of June, 2000 is shown in the lower panel of Figure B2, for which the vertical axis has been re-scaled to the maximum observed range of RFI (about 600 counts for AMSU-B channel 4).

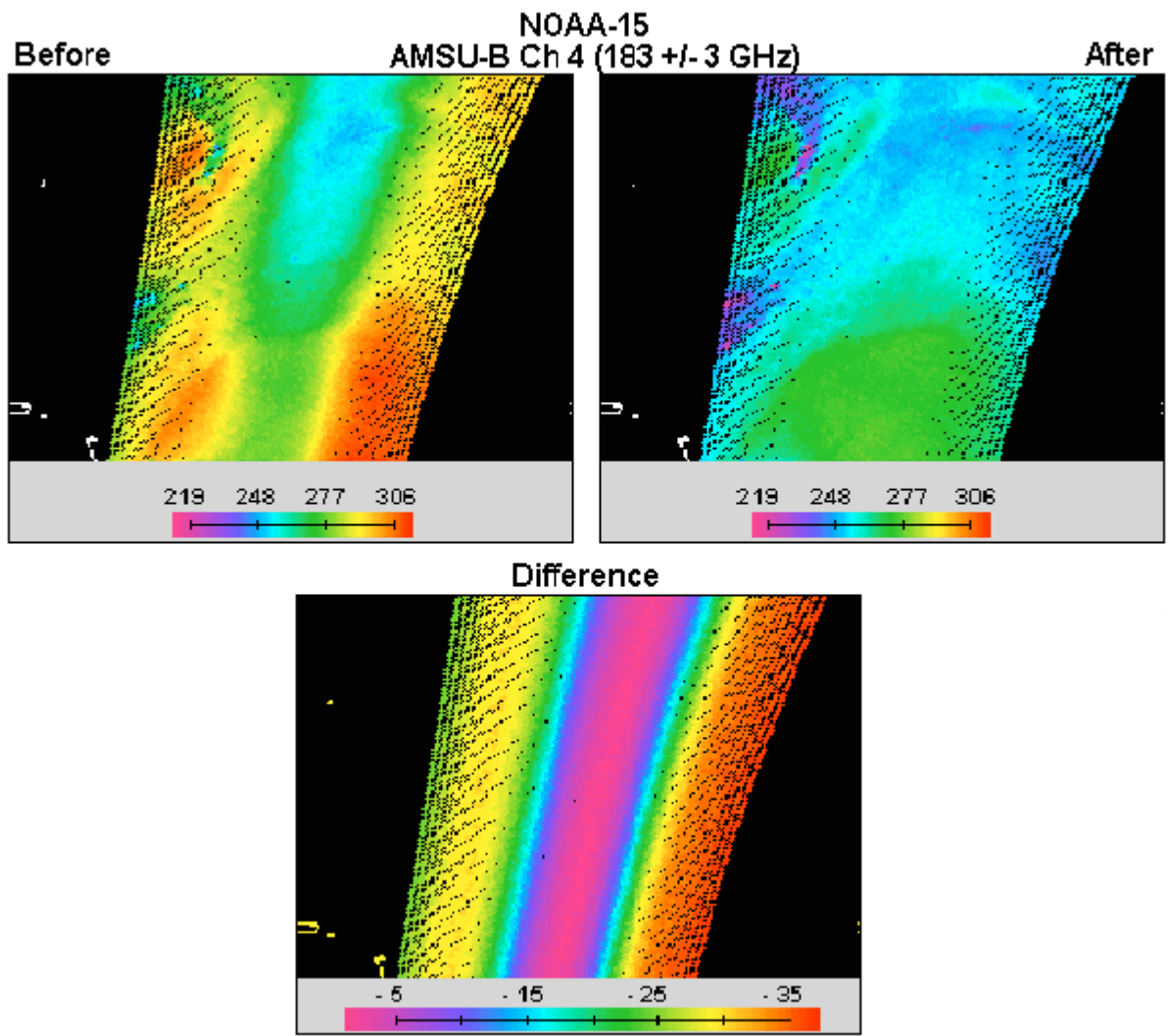


Figure B1: AMSU-B radiance temperature measurements ($^{\circ}\text{K}$) for channel 4 ($183 \pm 3\text{GHz}$) before (upper left) and after (upper right) RFI corrections, and the magnitude ($^{\circ}\text{K}$) of the correction (lower) for NOAA-15 during May, 2001.

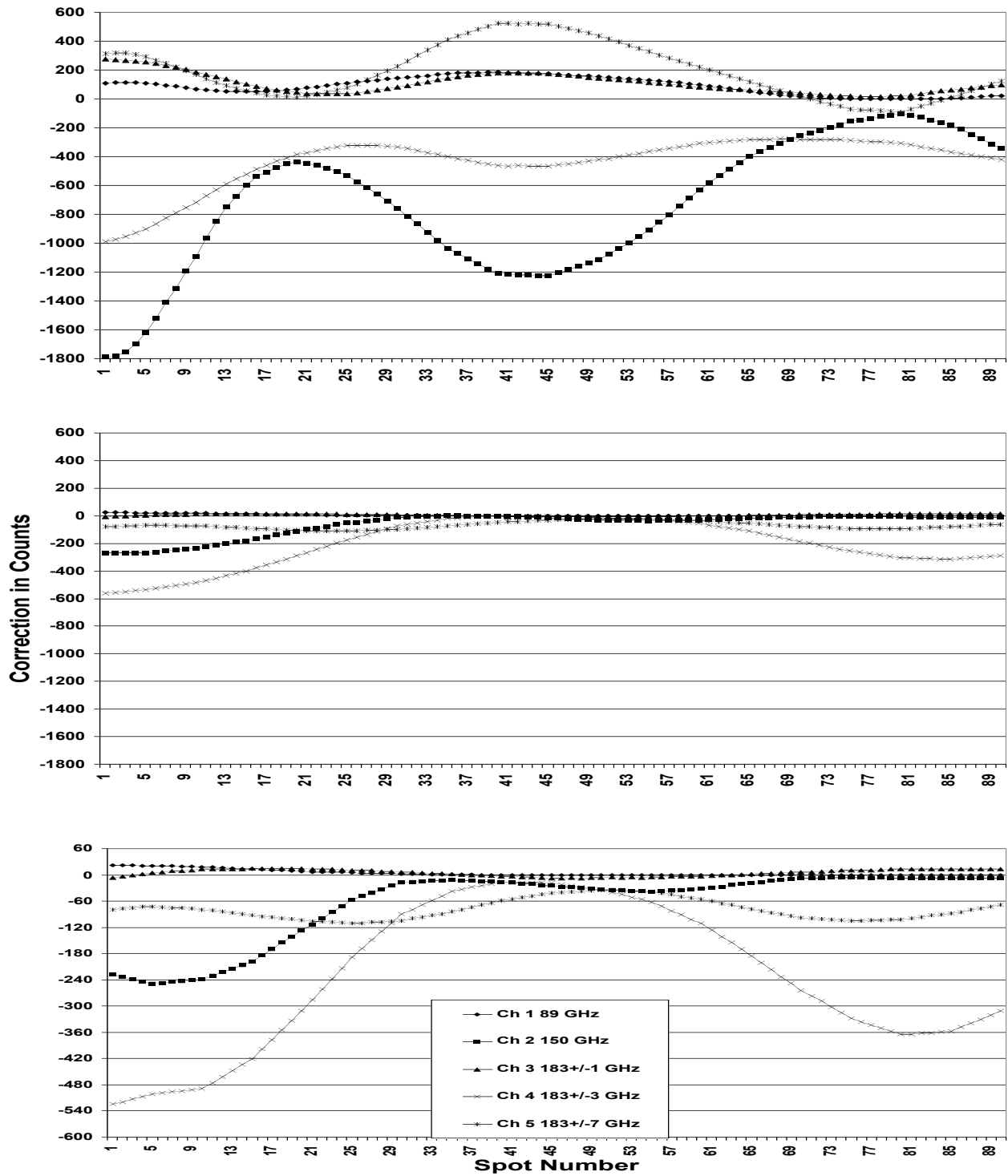


Figure B2: NOAA-15 correction values in counts (vertical axis) for each of the ninety-one (91) AMSU-B fov positions across the scan (horizontal axis) for channels 1 (89GHz), 2 (150GHz), 3 (183 ± 1 GHz), 4 (183 ± 3 GHz) and 5 (183 ± 7 GHz) before (top) and after (middle) September 28, 1999, and for enhanced vertical scale after June 20, 2000.

References

- Allegrino, A., A.L. Reale, M.W. Chalfant and D.Q.Wark, 1999: *Application of limb adjustment techniques for polar orbiting sounding data*. Technical Proceedings of the 10th International TOVS Study Conference, Jan 26- Feb 2, Boulder, Colorado, USA., 1-10.
- Andersson, E., A. Hollingsworth, G. Kelley, P. Lonngberg, J. Pailleux, and Z. Zhang, 1991: *Global observing system experiments on operational statistical retrievals of satellite sounding data*. Monthly Weather Review, AMS, Vol. 119, No. 8, 1852-1864.
- Atkinson, N.C., 2000: *Calibration, monitoring and validation of AMSU-B*. 33rd Committee on Space Research (COSPAR) Scientific Assembly, Warsaw, 16-23 July, to be published in Advances in Space Research.
- Atkinson, N.C., 1999: *Calibration and in-orbit performance of AMSU-B*. Technical Proceedings of the ECMWF/EUMETSAT Workshop on Use of ATOVS Data for NWP Assimilation, 2-5 November, 105-108.
- Bergman, K.H., 1978: *Observational errors in optimum interpolation analysis*. Bull. Amer. Meteor. Soc., Vol. 51, pp 1603-1611.
- Brown, C.E., Caldwell, J., Sief, K. Carey, R., and Reale, A., 1992: *EDGE: A PC based display system for visualizing NOAA environmental data*. 8th International Conference on Interactive Information and Processing Systems for Meteorology, Oceanography and Hydrology. Preprint Volume, AMS, Atlanta Georgia. ***
- Brown, C.E., A.L.Reale and M.W. Chalfant, 1991: *An improved image processing display system for the evaluation of satellite based meteorological products*. 7th International Conference on Interactive Information and processing Systems for Meteorology, Hydrology and Oceanography, Preprint Volume, AMS, New Orleans, La., 425-430.
- Brown, C.E., K.B. Fakhrai, M.Liu, A. Swaroop, and A. Reale, 1988: *An image processing display system for evaluation of operational meteorological products*. 5th International Conference on Interactive Information and processing Systems for Meteorology, Hydrology and Oceanography, Preprint Volume, AMS, Anaheim, Ca., 104-107.
- Caplan, P., J. Derber, W. Gemmill, S. Hong, H. Pan, and D. Parrish, 1997: *Changes to the NCEP operational medium-range forecast model analysis-forecast system*. Weather and Forecast, 12, Sept., pp 581-594.
- Chalfant, M.W., A. Reale, and F. Tilley, 1999: *Status of NOAA Advanced Microwave Sounding Unit-B products*. Technical Proceedings of the 10th International TOVS Study Conference, Jan 26- Feb 2, Boulder, Colorado, USA., 60-71.
- Crone, L.J., L.M. McMillin, and D.S. Crosby, 1996: *Constrained Regression in satellite meteorology*. Journal of Applied Meteorology, AMS, Vol 35, No. 11, 2023-2035.

- Crosby, D.S., H.E. Fleming, and D.Q. Wark, 1973: *Covariance matrices and means of atmospheric Planck functions for applications to temperature sounding from satellite measurements*. J. Atmos. Sci., Vol 30, No. 1, 141-144.
- Daniels, J.M., M.D. Goldberg, H.E. Fleming, B. Katz, W.E. Baker and D.G. Deaven, 1988: *Asatellite retrieval/forecast model interactive assimilation system*. 12th Conference on Weather Analysis and Forecasting, AMS, Monterey, California.
- Derber, J.C., and W.S. Wu, 1998: *The use of TOVS cloud-cleared radiance in the NCEP SSI analysis system*. Mon. Wea. Rev., 126, 2287-2299.
- Dey, C., R. Peterson, B. Ballish, P. Caplan, G. White, H. Fleming, A. Reale, D. Gray, M. Goldberg, and J. Daniels, 1989: *An evaluation of NESDIS TOVS physical retrievals using data impact studies*. NOAA Technical Memorandum NWS NMC 69, U.S. Dept. Of Commerce, Washington D.C., 25 pp.
- Eyre, J.R. and M.J. Uddstrom, 1993: *A report on the seventh international TOVS study conference*, 10-16 February, Igyls, Austria, 47 pp..
- Ferguson, M.P., and A.L. Reale, 2000: *Cloud detection techniques in NESDIS Advanced-TOVS sounding products systems*. 10th Conference on Satellite Meteorology and Oceanography, 9-14 January, Long Beach, Ca., 252-254.e
- Ferrare, R.A., S.H. Melfi, D.N. Whiteman, K.D. Evans, F.J. Schmidlin, and D. O’C. Starr, 1995. *A comparison of water vapor measurements made by Raman lidar and radiosondes*. J. Atmos. and Oceanic Tech., Vol. 12, 1177-1195.
- Finger F.G., M.E. Gelman, J.D. Wild, M.L. Chanin, A. Hauchecorne, and A.J. Miller, 1993: *Evaluation of NMC upper-stratospheric temperature analysis using rocketsonde and lidar data*. Bull. Amer. Meteor. Soc., Vol 34, No. 5, 789-799.
- Fleming, H.E., et. al., 1991: *The forward problem and corrections for the SSM/T satellite microwave temperature sounder*. IEEE Transactions on Geoscience and remote Sensing, Vol. 29, No. 4, 571-584.
- Fleming, H.E., D.S. Crosby, and A.C. Neuendorffer, 1986: *Correction of satellite temperature retrieval errors due to errors in atmospheric transmittances*. Journal of Climate and Applied Meteorology, Vol 25, No. 6, 869-882.
- Goldberg, M.D., 1999: *Generation of retrieval products from AMSU-A: methodology and validation*. Technical Proceedings of the 10th International TOVS Study Conference, Jan 26- Feb 2, Boulder, Colorado, USA., 219-229.
- Goldberg, M.D., 2001: *The limb adjustment of AMSU-A observations: methodology and validation*. Journal of Applied Meteorology, Vol. 40, 70-83.

- Goldberg, M, J. Daniels and H. Fleming, 1988: *A method for obtaining an improved initial approximation for the temperature/moisture retrieval problem*. Preprints, 3rd Conference on satellite Meteorology and Oceanography, Anaheim, Ca, 16-19.
- Goldberg, M.D., A. Reale and G. Kratz, 1998: *The use of pattern recognition to derive SSM/T2 moisture retrievals*. Adv. Space res., Vol. 21, 385-398.
- Goodrum, G, K.B. Kidwell, and W. Winston, 2000: *NOAA KLM users guide: September 2000 Revision*. U.S. Department of Commerce, NOAA, NESDIS, NCDC, Climate Services Division, Satellite Services Branch, Suitland, MD.
- Grody, N., et. al., 1999: *Applications of AMSU for obtaining water vapor, cloud liquid water, precipitation, snow cover and sea ice concentration*. Technical Proceedings of the 10th International TOV Study Conference, Jan 26- Feb 2, Boulder, Colorado, 230-240.
- Grody, N.C., 1991: *Classification of snowcover and precipitation using the special sensor microwave imager*. J. Geophys. Res., Vol 96, pp 7423-7435.
- Kalnay, E., M. Kanamitsu, and W.E. Baker, 1990: *Global numerical weather prediction at National Meteorological Center*. Bull. Amer. Meteor. Soc., Vol 71, pp 1410-1428.
- Kelly, G., E. Andersson, A. Hollingsworth, P. Lonnberg, J. Pailleux, and Z. Zhang, 1991: *Quality control of operational physical retrievals of satellite sounding data*. Mon. Wea. Rev., Amer. Meteor. Soc., Vol 119, No. 8, 1866-1880.
- Kelly, G., T. McNally and J. Eyre, 1992: *OSE experiments with 1D-Var, NESDIS, and NOSATEMS*. Research Department Memorandum, ECMWF, Reading England, May 11, 14 pp.
- Kidwell, K.B., 1998: *NOAA polar orbiter data user's guide (TIROS-N, NOAA-6, NOAA-7, NOAA-8, NOAA-9, NOAA-10, NOAA-11, NOAA-12, NOAA-13 and NOAA-14): November 1998 revision*. U.S. Department of Commerce, NOAA, NESDIS, NCDC, Climate Services Division, Satellite Services Branch, Suitland, MD.
- McMillin, L.M., L. Crone and T.J. Kleespies, 1995: *Atmospheric transmittances of an absorbing gas. 5.Improvements to the OPTRAN approach*. Appl. Opt., 34, 8396-8399
- McMillin, L.M., S.S. Zhou, and S.K. Yang, 1994: *An improved cloud retrieval algorithm using HIRS2-MSU radiance measurements*. J. Appl. Meteor., Vol. 33, pp 195-211.
- McMillin, L.M., and M. Uddstrom, 1992: *A procedure for correcting radiosonde reports for radiation errors*. Journal of Atmospheric and Oceanic Technology, Vol. 9, No. 6, pp 802-811.
- McMillin, L.M., L.J. Crone and D.S. Crosby, 1989: *Adjusting satellite radiance by regression with an orthogonal transformation to a prior estimate*. Jour. Appl. Meteor., Vol 28, No 9, 969-975.

- McMillin, L.M., M.E. Gelman, A. Sanyal, and M. Sylva, 1988: *A method for the use of satellite retrievals as a transfer standard to determine systematic radiosonde errors*. Mon. Wea. Rev., Vol. 116, pp 1091-1102.
- McMillin, L.M., and C. Dean, 1982: *Evaluation of a new operational technique for producing clear radiance*. J. Appl. Meteor., 12, pp 1005-1014.
- Neuendorffer, A.C., 1996: *Ozone monitoring with TIROS-N operational vertical sounders*. Journal of Geophysical Research, Vol 101, No. D13, 18807-18828.
- Pettey, M., and C.E. Brown, 2000: *The polar orbiting satellite sounding evaluator*. 16th International Conference on Interactive Information and Processing Systems for Meteorology, Hydrology and Oceanography, Preprint Volume, AMS, Anaheim, Ca., 366-368.
- Reale, A.L., M.W. Chalfant, and L.M. Wilson, 2000a: *NESDIS advanced TOVS sounding products*. 10th Conference on Satellite Meteorology and Oceanography, 9-14 January, Long Beach, Ca., 259-262.
- Reale, A.L., M.W. Chalfant, and F.H. Tilley, 2000b: *NESDIS moisture sounding products from AMSU-B and SSM/T2*. 10th Conference on Satellite Meteorology and Oceanography, 9-14 January, Long Beach, Ca., 263-266.
- Reale, A., M. Chalfant and L. Wilson, 1999a: *Scientific status of NOAA advanced TOVS sounding products*. Technical Proceedings of the 10th International TOVS Study Conference, Jan 26- Feb 2, Boulder, Colorado, USA., 437-448.
- Reale, A., M. Chalfant and L. Wilson, 1999b: *Scientific status of NESDIS advanced TOVS sounding products*. Technical Proceedings of the ECMWF/EUMETSAT Workshop on Use of ATOVS Data for NWP Assimilation, 2-5 November, 1999, 153-160
- Reale, A.L., M.W. Chalfant, and E. Brown, 1998: *NESDIS operational sounding product systems for NOAA and DMSP polar orbiting satellites*. 9th Conference on Satellite Meteorology and Oceanography, 25-29 May, Paris, France, Vol 2, 600-603.
- Reale, A.L., H.J. Bloom, and D.R. Donahue, 1995a: *Scientific status for NOAA and DMSP operational soundings*. Technical proceeding of the 8th International TOVS Study Conference, Queenstown, New Zealand, 395-404.
- Reale, A.L., H.J. Bloom, and T.J. Gardner, 1995b: *Revised TOVS (RTOVS) sounding system status*. Technical proceeding of the 8th International TOVS Study Conference, Queenstown, New Zealand, 417-422.
- Reale, A.L. 1995c: *Departures between derived satellite soundings and numerical weather forecasts: present and future*. Technical proceeding of the 8th International TOVS Study Conference, Queenstown, New Zealand, 395-404.

- Reale, A.L., M.W. Chalfant, R.V. Wagoner and T.J. Gardner, 1994: *TOVS Operational Sounding Upgrades: 1990-1992*. NOAA Technical Report NESDIS 76, U.S. Dept of Comm., Washington, D.C., 67 pp.
- Reale, A.L., 1993: *Scientific status for NOAA and DMSP operational soundings*. Technical Proceedings of the 7th International TOVS Study Conference, Igls, Austria, 392-403.
- Reale, A., H. Fleming, D. Wark, C. Novak, M. Gelman, F. Zbar, J. Neilon, and H. Bloom, 1990: *Baseline upper air network final report*. NOAA Technical Report NESDIS 52, U.S. Dept. Of Commerce, Washington D.C., 57 pp.
- Reale, A. L., M. D. Goldberg, and J. M. Daniels, 1989: *Operational TOVS soundings using a physical retrieval approach*. 12th Canadian Symposium on Remote Sensing, Vancouver, B.C., Vol 4, 2653-2657.
- Reale, A.L., D. G. Gray, M. W. Chalfant, A. Swaroop, and A. Nappi, 1986: *Higher resolution operational satellite retrievals*. Preprint Volume, 2nd Conference on Satellite Meteorology/Remote Sensing and Applications, Williamsburg, Va., 16-19.
- Schmidlin, F.J., 1998: *Radiosonde relative humidity sensor performance: the WMO intercomparison-Sept 1995*. 10th Symposium on Meteorological Observations and Instrumentation, AMS, 11-16 January, Phoenix Az., 68-71.
- Smith, W.L., H.M. Woolf, C.M. Hayden, D.Q. Wark, A.J. Schreiner and J.F. LeMarshall, 1984: *The physical retrieval TOVS export package*. Proc. Of the First International TOVS Study Conference, Madison, Wi., Cooperative Institute for Meteorological Satellite Studies, 227-278.
- Smith, W.L., H.M. Woolf, C.M. Hayden, D.Q. Wark, and L.M. McMillin, 1979: *The TIROS-N operational vertical sounder*. Bull. Amer. Soc., 60, 1177-1187.
- Smith, W.L., and H.M. Woolf, 1976: *The use of eigenvectors of statistical covariance matrices for interpreting satellite sounding radiometer observations*. J. Atmos. Sci., Vol 33, 1127-1140.
- Smith, W. L., 1968: *An improved method for calculating tropospheric temperature and moisture from satellite radiometer measurements*. Mon. Wea. Rev., Vol 96, 387-396.
- Soden, B.J., and J.R. Lanzante, 1996: *An assessment of satellite and radiosonde climatologies of upper tropospheric water vapor*. J. Climate, Vol. 9, 1235-1250.
- Sullivan, J., and A.Gruber, 1990: *Horizontal Covariance of NOAA-10 satellite temperature errors*. Preprints Volume of 5th Conference on Satellite Meteorology and Oceanography, AMS, 3-7 September, London, England, 408-413.
- Tilley, F.H., M.E. Pettey, M.P. Ferguson, and A.L. Reale, 2000: *Use of radiosondes in NESDIS advanced-TOVS (ATOVS) sounding products*. 10th Conference on Satellite Meteorology and Oceanography, 9-14 January, Long Beach, Ca., 255-258.

- Uddstrom, M.J., and L.M. McMillin, 1994a: *System noise in the NESDIS TOVS forward model. Part I: specification*. Jour. Appl. Meteor., Vol. 8, No. 33, pp 919-929.
- Uddstrom, M.J., and L.M. McMillin, 1994b: *System noise in the NESDIS TOVS forward model. Part II: consequences*. Jour. Appl. Meteor., Vol. 8, No. 33, pp 930-939.
- Wallace J.M., and P.V. Hobbs, 1977: *Atmospheric science an introductory survey*. Academic Press Inc. (London) Ltd, pp 467.
- Walton, C.C., W.G. Pichel and J.F. Sapper, 1998: *The development and operational application of nonlinear algorithms for the measurement of sea surface temperatures with the NOAA polar-orbiting environmental satellites*. Journal of Geophysical Research, Vol. 103, No. C12, 27999-28012.
- Wang, J., H.L. Cole, and D.J. Carlson, 2001: *Performance of Vaisala RS80 radiosonde on measuring upper tropospheric humidity after corrections*. 11th Symposium on Meteorological Observations and Instrumentation, 14-19 January, Albuquerque, NM.
- Wark, D.W., 1993: *Adjustment of TIROS operational vertical sounder data to a vertical view*. NOAA Technical Report NESDIS-64, U.S. Dept. Of Comm., Washington D.C., 36 pp.
- Weng, F., and N. Grody, 1994: *Retrieval of cloud liquid water using the special sensor microwave imager (SSM/I)*. J. Geophys. Res., Vol 99, 25535-25551.
- Werbowetzki, A., 1981: *Atmospheric sounding user's guide*. NOAA Technical Report NESS 83, U.S. Dept. Of Comm, Washington D.C., 82 pp.
- Wickham P.G., 1970: *The practice of weather forecasting*. Her Majesty's Stationary Office, London, 187 pp.
- Wu, X., J.J. Bates and S.J.S. Khalsa, 1993: *A climatology of the water vapor band brightness temperatures from NOAA operational satellites*. Journal of Climate, Vol 6, No 7, 1282-1300.
- Yang, S.K., S.S. Zhou, L.M. McMillin, and K.A. Campana, 1996: *Characteristics of the NOAA/NESDIS cloud retrieval algorithm using HIRS-MSU radiances measurements*. Journal of Applied Meteorology, AMS, Vol 35, No. 11, 1980-1990.

List of Illustrations

- Figure 1 - System schematic diagram of Orbital processing (red), and the Daily (green) and Weekly (blue) Offline support systems for ATOVS-A and ATOVS-B sounding products
- Figure 2 - Precipitation detection parameters of Cloud Liquid Water (mm) (upper left) and median filter edits (upper right), the final set of edits for AMSU-A fov (lower right), and AMSU channel 5 radiance temperature ($^{\circ}\text{K}$) measurements (lower left), composited from 16Z to 23Z on September 6, 2000 for NOAA-15
- Figure 3 - HIRS channel 8 radiance temperature ($^{\circ}\text{K}$) measurements (upper left), the corresponding cloud test differences ($^{\circ}\text{K}$) for "SST - STEH18" (upper right) and "PAMSU5 (LW) - AMSU5" (lower right) tests as defined in Table 1, and the resulting cloud mask (lower left), composited from 18Z on September 6, to 01Z on September 7, 2000, for NOAA-15
- Figure 4 - The first guess and retrieval sequence for one channel and level, showing AMSU-A channel 6 radiance temperature measurements ($^{\circ}\text{K}$) (upper left), corresponding first guess measurements (upper right) and 500 mb temperatures (lower right) ($^{\circ}\text{K}$), and 500 mb final sounding temperatures ($^{\circ}\text{K}$) at 500 mb, composited from 18Z on September 6, to 01Z on September 7, 2000
- Figure 5 - A typical global distribution of radiosonde reports from a single day
- Figure 6 - The global distribution of clear and cloudy collocations stored on the First Guess Libraries from NOAA-15 observed on September 6, 2000
- Figure 7 - Mean temperature profiles ($^{\circ}\text{K}$) for Polar (solid blue) and Tropical (solid red) atmospheres, overlaid by corresponding weighting function curves for HIRS/3 channel 7 (dashed), and (in ascending order) by AMSU-A channels 5, 8 and 13 for NOAA-16, as computed for the Polar (blue) and Tropical (red) atmospheres versus geopotential height (m) (vertical axis), with the temperature ($^{\circ}\text{K}$) and weight values defined along the upper and lower horizontal axis
- Figure 8 - Bias adjusted radiance temperature measurements ($^{\circ}\text{K}$) for the AMSU-B upper tropospheric moisture channel at 183 ± 1 GHz., onboard NOAA-15, and the corresponding magnitude of adjustments (lower), composited from 16Z on September 6 to 05Z on September 7, 2000
- Figure 9 - Satellite minus radiosonde mean and standard deviation differences ($^{\circ}\text{K}$) for ATOVS-A Clear (left) and Cloudy (right) for first guess (thin) and final (thick) temperature soundings, respectively, from 60N to 60S during a 7-day period in September, 2000. Pressure (mb) is indicated on the left axis with corresponding sample size on the right

- Figure 10 - Satellite minus radiosonde mean and standard deviation differences (%) for ATOVS-B first guess (thin) and final (thick) moisture soundings from the 90N to 30N (left) and 30N to 30S regions, respectively, during a 7-day period in September, 2000. Differences are percentages of the mean mixing ratio profiles (g/kg) shown on the inside of the left axis, with pressure on the outer left axis and sample size on the right axis
- Figure 11 - AMSU-A radiance temperature measurements ($^{\circ}\text{K}$) for channels 6 and 5, and corresponding Satellite minus NWP forecast difference ($^{\circ}\text{K}$) fields for upper (500 to 300 mb) and lower (1000 to 700 mb) tropospheric layers, respectively, composited from 18Z to 22Z on September 6, 2000 for NOAA-15
- Figure 12 - AMSU-A radiance temperature measurements ($^{\circ}\text{K}$) for channels 7 and 8, and corresponding satellite sounding temperature fields ($^{\circ}\text{K}$) at 250 and 200 mb, composited from 18Z to 22Z on September 6, 2000, for NOAA-15
- Figure 13 - EMC 12-hour averaged fields for analyzed 250 mb temperature ($^{\circ}\text{C}$) (upper), tropopause pressure (mb) (middle), and 250 mb winds (knots) (lower) for 06Z on September 7, 2000
- Figure 14 - HIRS channel 8 radiance temperature ($^{\circ}\text{K}$) measurements (upper left), derived cloud-top pressure (mb) (upper right), and concurrent AMSU-B radiance temperature measurements ($^{\circ}\text{K}$) at 183 ± 3 GHz. (lower left) and derived moisture (g/kg) at 620 mb (lower right), composited from 18Z to 22Z on September 6, 2000 for NOAA-15
- Figure 15 - AMSU-B radiance temperature measurements ($^{\circ}\text{K}$) at 183 ± 1 GHz. (left panels) and derived 500 mb moisture (g/kg) for composited fields from approximately 18Z to 0Z (upper), and 16 Z to 4Z (lower) on September 6 and 7, 2000 for NOAA-15
- Figure 16 - AMSU-A radiance temperature measurements ($^{\circ}\text{K}$) for channel 13 (upper left) and derived temperatures ($^{\circ}\text{K}$) at 5mb for NOAA-15 (upper right) and for NOAA-14 (lower left), and NOAA-15 minus NOAA-14 temperature difference at 5 mb, composited for the period 16 Z to 05Z on September 6 and 7, 2000
- Figure B1 - AMSU-B radiance temperature measurements ($^{\circ}\text{K}$) for channel 4 ($183 \pm 3\text{GHz}$) before (upper left) and after (upper right) RFI corrections, and the magnitude ($^{\circ}\text{K}$) of the correction (lower) for NOAA-15 during May, 2001
- Figure B2 - NOAA-15 correction values in counts (vertical axis) for each of the ninety-one (91) AMSU-B fov positions across the scan (horizontal axis) for channels 1 (89GHz), 2 (150GHz), 3 ($183 \pm 1\text{GHz}$), 4 ($183 \pm 3\text{GHz}$) and 5 ($183 \pm 7\text{GHz}$) before (top) and after (middle) September 28, 1999, and for enhanced vertical scale after June 20, 2000

List of Tables

- Table 1 - Regression based cloud detection tests, thresholds and application constraints for ATOVS-A, NOAA-15, during September-2000. The prefixes “STE” and “P” refer to Surface Temperature Estimates and Predicted parameters
- Table 2 - Non-Regression, Restoral and Adjacent Spot cloud detection tests, thresholds and application constraints for ATOVS-A, NOAA-15, during September 2000
- Table 3 - First Guess (FG) and Retrieval (RE) Channel Combinations (CC) for ATOVS-A Sounding Types
- Table 4 - First Guess (FG) and Retrieval (RE) Channel Combinations (CC) for ATOVS-B Sounding Types
- Table 5 - The 23 categories (CAT) and associated sampling criteria and characteristics for the MDB and First Guess Libraries of ATOVS-A on September 6, 2000
- Table 6 - Predictand, predictor(s), parameter name and sampling constraints for regression coefficients used in cloud detection
- Table A1 - Table A1 shows the channel number, center frequency (GHz), the atmospheric pressure of peak sensitivity, and atmospheric product retrieved for each of the AMSU-A radiometer channels onboard NOAA-15
- Table A2 - Table A2 shows the channel number, center frequency (cm^{-1}), the atmospheric pressure of peak sensitivity, and atmospheric product retrieved for each of the HIRS/3 radiometer channels onboard NOAA-15
- Table A3a - This table shows the channel number, center frequency, the atmospheric pressure of peak sensitivity, and atmospheric product retrieved for each of the AVHRR radiometer channels onboard NOAA-15
- Table A3b - This table shows the channel number, center frequency, the atmospheric pressure of peak sensitivity, and atmospheric product retrieved for each of the AMSU-B radiometer channels onboard NOAA-15